STRUCTURAL AND FUNCTIONAL ANALYSIS OF INTRA-CELLULAR TRANSPORT BETWEEN GOLGI APPARATUS AND ENDOSOME/LYSOSOME SYSTEM USING SYNCHROTRON RADIATION

MICHIO INOUE

Department of Materials Structure Science
School of High Energy Accelerator Science
The Graduate University for Advanced Studies

2004
(School Year)

Abbreviations

AAA	ATPases associated with diverse cellular activities
AP	adaptor protein
CA	carbonic anhydrase
E. coli	*Escherichia coli*
ER	endoplasmic reticulum
ESCRT	endosomal sorting complex required for transport
GAE	γ-adaptin ear
γ1-ear	γ-ear domain of AP-1
GAT	GGA and Tom1
GGA	Golgi-localizing, γ-adaptin ear homology domain, ARF-binding
GST	glutathione S-transferase
HEPES	2-[4-(2-Hydroxyethyl)-1-piperazinyl]ethanesulfonic acid
K_d	dissociation constant
MES	2-morpholinoethanesulfonic acid
MPR	mannose 6-phosphate receptor
MVB	multivesicular body
PEG	polyethylene glycol

PSPC position sensitive proportional counter

R_g radius of gyration

r.m.s.d. root mean square deviations

SAXS small angle X-ray scattering

S. cerevisiae *Saccharomyces cerevisiae*

SDS sodium dodecyl sulfate

SKD1 suppressor of K^+ transport growth defect 1

SPR surface plasmon resonance

TGN *trans*-Golgi network

Tris tris hydroxymethyl aminomethane

VHS Vps27p/Hrs/STAM

vps vacuolar protein sorting

Summary

GGA (Golgi-localizing, γ-adaptin ear homology domain, ARF-binding) proteins and adaptor protein (AP) complex AP-1 regulate membrane traffic between TGN (*trans*-Golgi network) and endosomes. The GAE (γ-adaptin ear) domains of GGA proteins share sequence homology with the γ1-ear (γ-ear domain of AP-1). Both the GGA1-GAE and γ1-ear interact with the consensus acidic phenylalanine motif of various accessory proteins. In addition, γ1-ear was found to interact with the WNSF motif of the GGA1-hinge region, although the WNSF motif deviates from the consensus sequence of the acidic phenylalanine motif. I report here that the GAE domain of GGA1 also interacts with the WNSF motif of its own hinge region, resulting in an autoinhibition of the interaction between GGA1-GAE and accessory proteins. The complex structure of GGA1-GAE with the GGA1-hinge peptide, which is determined by synchrotron X-ray crystallography, revealed that two aromatic rings of the WNSF motif locate on the hydrophobic groove surrounded by the aliphatic portions of the conserved arginine and lysine residues of GGA1-GAE. Furthermore, the interface is stabilized by an intermolecular β-sheet between the extended peptide backbone and β4-strand of GGA1-GAE. The interaction mode between GGA1-GAE and the GGA1-hinge peptide is similar to that of the previously reported structures of the

GGA-GAE/acidic phenylalanine motif complexes, suggesting possible competition between accessory proteins and the GGA1-hinge region at the same binding site of GGA1-GAE. The fluorescence quenching experiment suggested that GGA1-GAE interacts with the GGA1-hinge region and the accessory proteins can compete with the GGA1-hinge excluding/expelling from GGA1-GAE. Together with the previous observation that γ1-ear binds to the GGA1-hinge region, these suggest that the autoinhibition between the GGA1-hinge region and GGA1-GAE controls the clathrin mediated traffic pathway, through the competitive interaction with accessory proteins and AP-1.

Introduction

Clathrin-mediated membrane traffic between TGN (*trans*-Golgi network) and endosomes is regulated by GGA (Golgi-associated, γ-ear-containing, ARF-binding) proteins and AP (adaptor protein) complex AP-1. While AP-1 is a heterotetrameric complex, three GGA proteins (GGA1, 2 and 3) were found as a new family of homomonomeric adaptor proteins (Boman *et al.* 2000, Hirst *et al.* 2000, Dell'Angelica *et al.* 2000, Poussu *et al.* 2000, Takatsu *et al.* 2000). GGA proteins are composed of three domains and one flexible region: the N-terminal VHS (Vps27p/Hrs/STAM) domain which recognizes the consensus acidic phenylalanine motif of lysosomal cargo receptors such as MPR (mannose 6-phosphate receptors) (Nielsen *et al.* 2001, Puertollano *et al.* 2001a, Takatsu *et al.* 2001, Zhu *et al.* 2001), the GAT (GGA and Tom1) domain which interacts with the GTP-bound form of ARF on the TGN membrane (Boman *et al.* 2000, Dell'Angelica *et al.* 2000, Puertollano *et al.* 2001b, Takatsu *et al.* 2002, Zhdankina *et al.* 2001), the proline-rich hinge region which interacts with clathrin (Mullins *et al.* 2001, Puertollano *et al.* 2001b, Zhu *et al.* 2001) and the C-terminal GAE (γ-adaptin ear) domain which is homologous to the γ1-ear (γ-ear domain of AP-1) (Boman *et al.* 2000, Dell'Angelica *et al.* 2000, Hirst *et al.* 2000, Poussu *et al.* 2000, Takatsu *et al.* 2000).

Both GGA-GAEs and γ1-ear interact with a number of accessory proteins: γ-synergin (Hirst *et al.* 2000, Mills *et al.* 2003, Page *et al.* 1999, Takatsu *et al.* 2000), Rabaptin-5 (Hirst *et al.* 2000, Mattera *et al.* 2003), EpsinR (Kalthoff *et al.* 2002, Lui *et al.* 2003, Mills *et al.* 2003, Wasiak *et al.* 2002), ARFGAP1 (Hirst *et al.* 2003), and Snx9 (Hirst *et al.* 2003). Recently, the PEEDDFQDFQDA sequence in γ-synergin were shown to be prerequisite for γ1-ear binding and the TSGNGDFGDWSA sequence in EpsinR (Mills *et al.* 2003). The DFGPLV sequence of Rabaptin5 was identified as the binding sequence of GGA-GAEs and γ1-ear (Mattera *et al.* 2003). Furthermore, the DEEEDDDDEFSEFQ sequence of Ent3p and the DDDDDEFGDFQ sequence of Ent5p are shown to be the binding site of the yeast Gga2 GAE domain and γ1-ear (Duncan *et al.* 2003a). From these observations, the consensus acidic phenylalanine motif $[D/E][G/A]_{(0-1)}F[G/A][D/E]\Phi$ (Φ is a bulky hydrophobic residue) was proposed as a consensus sequence of the binding motif of both GGA-GAEs and γ1-ear (Duncan and Payne 2003b). Crystal structures of GGA1-GAE in complex with the p56 accessory protein peptide and GGA3-GAE in complex with the Rabaptin-5 peptide have been reported (Collins *et al.* 2003, Miller *et al.* 2003). Both the p56 and the Rabaptin-5 peptides contain the consensus acidic phenylalanine motif, and the two conserved aromatic side chains of the peptides are stuck into the two pockets of GGA-GAEs

composed of hydrophobic portion of the side chains of conserved arginine and lysine residues in the crystal structures.

In addition to the accessory proteins, γ1-ear also interacts with the GGA-hinge region, suggesting that AP-1 and GGA cooperatively recruit cargoes to clathrin-coated vesicles at TGN (Doray *et al.* 2002). Our and other laboratories recently identified the sequence ^{382}WNSF^{385} of the GGA1-hinge region as a binding site of γ1-ear (Bai *et al.* 2004, Yamada *et al.* 2005), although it deviates from the consensus acidic phenylalanine motif [D/E][G/A]$_{(0\text{-}1)}$F[G/A][D/E]Φ found in the accessory proteins (Duncan and Payne 2003b). I report here that GGA1-GAE interacts with not only the consensus acidic phenylalanine motif but also with the WNSF motif of the GGA1-hinge region *in vitro*. I determined the complex structures of GGA1-GAE and the GGA1-hinge peptide, which revealed that the interaction mode of the WNSF motif and GGA1-GAE is essentially the same as that of the accessory proteins. I found an autoinhibition between GGA1-GAE and the GGA1-hinge region, which is in competition with accessory proteins. Our laboratory has also determined the crystal structure of γ1-ear in complex with the GGA1-hinge peptide and with the consensus acidic phenylalanine motif peptide of γ-synergin (Yamada *et al.* 2005), which revealed that the same binding site of γ1-ear is used for both the WNSF motif and the consensus acidic phenylalanine

motif. I will discuss the autoregulation mechanism of GGA1 based on these results.

Experimental procedures

Protein expression and purification

A DNA fragment for the GAE domain (residues 507-639) of human GGA1 was cloned into the pGEX4T-2 plasmid (Amersham Biosciences) and expressed in *Escherichia coli* (*E. coli*) BL21(DE3) cells. The glutathione S-transferase (GST) fusion protein was purified with affinity chromatography using a glutathione Sepharose 4B column (Amersham Biosciences), and cleaved by thrombin protease (Amersham Biosciences). Then, GGA1-GAE was purified by Superdex 75 size-exclusion column (Amersham Biosciences) chromatography in 100 mM NaCl and 20 mM Tris-HCl (pH 8.0).

For the expression of GGA1-hinge—GAE construct, a DNA fragment for residues 350-639, which contains both the hinge region and the GAE domain of GGA1, was cloned into the pGEX4T-2 plasmid and the resultant construct was called as GGA1-hinge—GAE throughout this manuscript. For the fluorescence experiment, two of the three tryptophan residues were replaced by alanines (W444A and W636A) by site directed mutagenesis kit (Quick change, Stratagene). In addition to the above two mutations, K611Q mutation was introduced to GGA1-hinge—GAE as a ligand binding-deficient mutant. Both constructs were expressed in *E. coli* BL21(DE3) cells

and purified by affinity chromatography using a glutathione Sepharose 4B column, and cleaved by thrombin, and further purified by a MonoQ anion exchange column with a linear gradient of 0-500 mM NaCl in 40 mM HEPES (pH 7.0).

Crystallization and data collection

All crystallization experiments were performed using a hanging-drop vapor diffusion method at 293 K. All crystallization reagents used were purchased from Hampton Research (USA) and deCODE genetics (USA). Crystals of GGA1-GAE ($0.05\times0.05\times0.3$ mm^3) were obtained using 15 mg ml^{-1} protein and a reservoir solution containing 20 % (wt./vol.) PEG3350 and 120 mM di-ammonium tartrate after a week at 293 K (Fig.1-1A). The synthetic GGA1-hinge peptide which has the WNSF motif (^{376}SLDGTG<u>WNSF</u>QSS^{388}) and the DDFGDF peptide which has the consensus acidic phenylalanine motif were purchased from TORAY Research Center (Japan) for co-crystallization with GGA1-GAE. Crystals of the complex between GGA1-GAE and the GGA1-hinge peptide ($0.3\times0.3\times0.6$ mm^3) (Fig.1-1B) and that between GGA1-GAE and the DDFGDF peptide ($0.05\times0.05\times0.1$ mm^3) (Fig.1-1C) were obtained after a week, using a 1:5 molar ratio mixture of GGA1-GAE (15 mg ml^{-1}) and the peptides.The reservoir solutions contain 20 % (wt./vol.) PEG3350, 120 mM

di-ammonium tartrate and 20 % (wt./vol.) PEG3350, 100 mM calcium acetate, 100 mM MES (pH 6.0), respectively.

The data sets of apo-form GGA1-GAE and the complex of GGA1-GAE with the GGA1-hinge peptide were collected at beamline AR-NW12 at the Photon Factory (Tsukuba, Japan). The data set of the complex with the DDFGDF peptide was collected at beamline BL38B1 at SPring-8 (Harima, Japan). All data sets were collected under cryogenic conditions with crystals soaked in a cryoprotectant solution containing 15 % (wt./vol.) glycerol and cooled at 100 K in a nitrogen gas stream. The diffraction data were integrated and scaled with the program HKL2000 (Otwinowski 1997).

Structure determination and refinement

The crystal structure of apo-form GGA1-GAE was solved by the molecular replacement method with the program MOLREP (Vagin *et al.* 1997) using the structure of human γ1-ear (PDB accession number: 1IU1 (Nogi *et al.* 2002)) as a search model. The model was refined using CNS (Brünger *et al.* 1998) and REFMAC5 (Murshudov *et al.* 1997) for the resolution range 50-2.3 Å. The manual adjustments of the model were performed using Turbo-FRODO (Roussel *et al.* 1991). The crystal contains

four GGA1-GAE molecules in an asymmetric unit; molecule A (residues 511-639), molecule B (residues 511-636), molecule C (residues 507-510 and 512-639) and molecule D (residues 511-639). The final model has an *R*-factor of 22.0% and R_{free} of 26.0%.

The crystal structure of GGA1-GAE in complex with the GGA1-hinge peptide was solved by the molecular replacement method with MOLREP (Vagin *et al.* 1997) using the structure of GGA1-GAE (molecule A) as a search model. The crystal contains four GGA1-GAE molecules; molecule A (residues 511-639), molecule B (residues 512-564, 570-604 and 609-639), molecule C (residues 512-639) and molecule D (residues 511-639) and two GGA1-hinge peptides; peptide P (residues ^{381}GWNSFQSS^{388}) and peptide Q (residues ^{381}GWN^{383} and ^{385}FQSS^{388}) in an asymmetric unit. Molecule A and C interact with peptide P and Q, respectively. The final model has an *R*-factor of 23.9% and R_{free} of 28.5% (resolution range 50-2.55 Å). The crystal structure of GGA1-GAE in complex with the DDFGDF peptide was solved by the molecular replacement method with MOLREP (Vagin *et al.* 1997) using the structure of GGA1-GAE (molecule A) as a search model. The crystal contains four GGA1-GAE molecules; molecule A (residues 512-639), molecule B (residues 512-639), molecule C (residues 513-534 and 536-637) and molecule D (residues 513-535 and

538-637) and one peptide; peptide P (residues FDGF) in an asymmetric unit. Molecule A interacts with peptide P. The final model has an *R*-factor of 21.2% and R_{free} of 25.9% (resolution range 50-2.65 Å). The statistics for the structure determination are summarized in Table 1-1. Root mean square deviations (r.m.s.d.) of the structure superpositions were calculated using the program LSQKAB (Kabsch 1976). Figures were prepared using the programs MolScript (Kraulis 1991), GRASP (Nicholls *et al.* 1991), Raster3D (Merritt 1997) and LIGPLOT (Wallace *et al.* 1995).

SAXS measurement of GGA1-GAE

The X-ray scattering data were collected at Photon Factory BL-10C in Tsukuba, Japan. The wavelength was set to 1.488 Å. Each sample solution (30 μL) was introduced into the thin-walled quartz capillary (path length of 1 mm) and fixed in the sample holder at 298 K. The protein concentrations of the solutions ranged from 3 mg/ml to 12 mg/ml. The scattered X-rays were recorded with an exposure time of 600 seconds at 900 mm from the sample position on PSPC (position sensitive proportional counter). The scattering X-rays recorded showed a one-dimensional intensity profile as a function of $Q=4\pi\sin\theta/\lambda$ (2θ: scattering vector, λ: wavelength of X ray). The $I(Q)$ data were corrected for the background scattering from the corresponding buffer

solution and for protein concentration. The origin of coordinate axes of scattering intensity (I(0)/conc.) was estimated from the Guinier plot [ln I (0) vs. Q^2] and the globularity of the protein was evaluated by the Kratky plot [I (Q)×Q^2 vs Q] (Kataoka *et al.* 1993).

SPR and fluorescence measurements

Binding affinities between GGA1-GAE or γ1-ear and ligand peptides were analyzed by SPR (surface plasmon resonance) using BIACORE2000 (BIACORE). The GST-fused peptides, whose constructs are described elsewhere (Yamada *in preparation*), were captured on a sensor chip CM5 (BIACORE) coated with anti-GST antibody (BIACORE). All SPR experiments were carried out in 150 mM NaCl and 10 mM HEPES (pH 7.5) buffer, at a flow rate of 20 μl min^{-1} at 293 K. SPR sensorgrams were analyzed using a program BIAevaluation 3.2 (BIACORE). Dissociation constants, K_d, were calculated using the steady-state affinity model.

Fluorescence spectra were analyzed by using fluorescence spectrophotometer, F-4500 (HITACHI). All fluorescence experiments were carried out in 100 mM NaCl and 20 mM HEPES (pH 7.0) buffer at 293 K. Fluorescence emission spectra of wild-type and K611Q mutant of GGA1-hinge—GAE were recorded at 20 μM protein

concentration. For the competition experiment, 1 mM DDFGDF peptide was added to the solution containing 2 μM of wild-type or K611Q mutant GGA1-hinge—GAE. In all fluorescent experiments, the exited wavelength was 295 nm and the emission spectra were recorded between 310 and 450 nm.

Results

Interaction between GGA1-GAE and the GGA1-hinge region

Our and other laboratories recently identified the sequence of ^{382}WNSF^{385} in the GGA1-hinge region as the binding site of γ1-ear (Bai *et al.* 2004, Yamada *et al.* 2005). I assumed that the GAE domain of GGA1 interacts with the WNSF motif of its own hinge region because GGA1-GAE is a structural and functional homologue of γ1-ear. To elucidate the hypothesis, I first measured the affinity between GGA1-GAE and the GGA1-hinge peptide by surface plasmon resonance (SPR), and compared it with the affinities between GGA1-GAE and accessory proteins.

The GAE-bindig sequences of γ-synergin (LADDFGEFSLFGE), EpsinR (GNGDFGDWSAFNQ) (Mills *et al.* 2003) and Rabaptin-5 (DESDFGPLVG) (Mattera *et al.* 2003) were fused to GST and immobilized on sensor chips. These sequences of accessory protein peptides includes the consensus acidic phenylalanine motif [D/E][G/A]$_{(0\text{-}1)}$F[G/A][D/E]Φ (Duncan and Payne 2003b). The interactions of the peptides with GGA1-GAE were measured by SPR (Fig. 1-2). The calculated dissociation constants (K_d) of GGA1-GAE for the γ-synergin and the EpsinR peptides were 75 μM and 110 μM, respectively (Table 1-2). These values are about one order of magnitude weaker than those of γ1-ear (5.1 μM and 22 μM, respectively) (Table 1-2).

The weaker bindings of γ-synergin and EpsinR to GGA1-GAE compared to γ1-ear was also reported (Hirst *et al.* 2003). On the other hand, GGA1-GAE and γ1-ear showed similar affinities (K_d values of 69 μM and 61 μM, respectively) for the Rabaptin-5 peptide (Table 1-2). The comparable binding affinity of GGA1-GAE and γ1-ear to Rabaptin-5 was also reported in a pull down experiment (Mattera *et al.* 2003).

Next, I measured the binding profiles of GGA1-GAE for the GST-fused WNSF motif of the GGA1-hinge region (^{379}GTGWNSFSQ^{387}). The WNSF motif deviates from the consensus acidic phenylalanine motif [D/E][G/A]$_{(0-1)}$F[G/A][D/E]Φ (Duncan and Payne 2003b) in the following two points. First, the WNSF motif does not contain acidic amino acid residues near the two bulky hydrophobic residues. Second, the conserved phenylalanine is replaced with tryptophan. Nevertheless, GGA1-GAE binds to the WNSF motif with K_d of 180 μM which is comparable to those with other accessory proteins (Fig. 1-2 and Table 1-2). This is the first observation that GGA1-GAE interacts with the GGA1-hinge region *in vitro*. This binding affinity is comparable to that between γ1-ear and the WNSF motif (K_d of 130 μM). In the case of the interaction between the WNSF motif and γ1-ear, the two bulky hydrophobic residues, tryptophan and phenylalanine of the WNSF motif, are the key residues for the interaction (Bai *et al.* 2004, Yamada *et al.* 2005). In my experiments, mutants of each

bulky hydrophobic residue to alanine (W283A or F285A) almost abolished the binding to GGA1-GAE (Fig.1-2). The interactions of these mutants to GGA1-GAE were too weak not to estimate the K_d values. Thus, the two bulky hydrophobic residues also play important roles in the interaction with GGA1-GAE.

Crystal structure of GGA1-GAE

To investigate the molecular mechanism of the interaction between GGA1-GAE and the WNSF motif, X-ray crystallographic studies were carried out. First, I determined the crystal structure of apo-form GGA1-GAE at 2.3 Å resolution by the molecular replacement method using the γ1-ear structure (Nogi *et al.* 2002) as a search model. The crystal structure shows that GGA1-GAE forms an immunoglobulin-like β-sandwich fold composed of two β-sheets (strands β1-β2-β3-β5-β6 and β4-β7-β8) and one α-helix at the C-terminus (Fig. 1-3A). The structures of the four molecules (molecule A, B, C and D) in the asymmetric unit are identified within a root mean square deviation (r.m.s.d.) of 0.67 Å for Cα atoms of the eight β-strands (residues 514-520, 522-530, 540-550, 552-564, 569-573, 591-599, 607-616 and 620-628). The GGA1-GAE structure is almost the same as the recently reported one which belongs to a different space group (Lui *et al.* 2003) with r.m.s.d. of 0.88Å. It is also similar to the

γ1-ear structure (Kent *et al.* 2002, Nogi *et al.* 2002) with r.m.s.d. of 1.34Å for Cα atoms of the eight β strands.

In the crystal, the four GGA1-GAE molecules in the asymmetric unit exist as two dimmers (molecules A-B and molecules C-D). The structures of two dimers in the asymmetric unit are identified within r.m.s.d. of 0.6 Å for Cα atoms of the eight β strands. Two dimmers are formed by face-to-face interactions of the β-sheets of two GGA1-GAE molecules related by pseudo two fold axis (Fig. 1-3A). Extensive interactions are observed between the two molecules through the β-sheet (composed of β1, β2, β3, β5 and β6) and two loops between β2 and β3 and between β5 and β6 (Fig. 1-3A). The buried surface areas upon dimerization are 2,913 $Å^2$ between molecule A and B, and 3,103 $Å^2$ between molecule C and D. Both dimers have predominantly hydrophobic contact area (Fig. 1-3B) and the dimerization seems to be caused by nonspecific hydrophobic interactions between the β-sheets of the two GGA1-GAE molecules. Although GGA1-GAE molecules forms a dimer through the face-to-face interaction of the β-sheet composed of β1, β2, β3, β5 and β6, another group has been reported that GGA1-GAE doesn't form a dimer in the different crystal lattice (Lui *et al.* 2003).

Dimer formation of GGA1-GAE in solution

I found that GGA1-GAE forms a dimer in the crystal, however, but it has not been reported whether GGA1 forms a monomer or dimer. To elucidate the oligomerization of GGA1-GAE in solution, I carried out small angle X-ray scattering (SAXS) experiment. Figure 1-4A shows Guinier plots of the solution scattering profile for GGA1-GAE. Carbonic anhydrase (CA) (Mw: 29,000) was used as a standard protein to estimate the molecular weight of GGA1-GAE. The result of Guinier fitting showed that the values of $I(0)$/conc. of GGA1-GAE were 5,326 (Fig. 1-4B) and that of CA was 6,068 (data not shown), respectively. From the values of $I(0)$/conc., the molecular weight of GGA1-GAE was calculated to be 25 kDa. This molecular weight was 1.7 times larger than that of GGA1-GAE calculated from the amino acid sequence. This suggests that GGA1-GAE exists as dimer in solution.

Next, I compared the shapes of Kratky plot calculated from monomer and dimer crystal structures to that from SAXS experiment (Fig. 1-5A). The integral intensity peak position of GGA1-GAE is about 0.09 Q ($Å^{-1}$), which suggests GGA1-GAE is a globular form. The shape of Kratky plot from SAXS experiment was very similar to that calculated from GGA1-GAE dimer but not monomer. Moreover, P(r) function of SAXS experiment was compared to those calculated from monomer and dimer crystal

structures. As shown in Fig. 1-5B, the peak and the shape of the P(r) function from dimer crystal structure coincide well to those from SAXS experiment. Gel filtration experiment said that elution time of GAE was not shown monomer size (data not shown). These results also suggest that GGA1-GAE forms dimer in solution.

Crystal structure of complex between GGA1-GAE and the GGA1-hinge peptide

Subsequently, I co-crystallized the complex between GGA1-GAE and the GGA1-hinge peptide (^{376}SLDGTGWNSFQSS^{388}) and determined its structure at 2.55 Å resolution by the molecular replacement method using the apo-form GGA1-GAE structure as a search model. An asymmetric unit contains four GGA1-GAE molecules (molecule A, molecule B, molecule C and molecule D) and two peptides (peptide P and peptide Q). Peptide P and Q bound to molecule A and C, respectively. I could not build peptide models on molecule B and D because of poor electron density at the putative binding site probably due to their low occupancies. The structures of molecules A, B, C and D in the asymmetric unit are identified within r.m.s.d. of 0.65 Å for Cα atoms of the eight β strands. The overall structures of the GGA1-GAE molecules in the complexes are almost the same as those of apo-form GGA1-GAE within highest r.m.s.d. of 0.96 Å for Cα atoms of eight β-strands.

Four GGA1-GAE molecules also form two dimmers in the crystal through the face-to-face interactions of the β-sheets opposite to the peptide-binding site of GGA1-GAE, in a similar manner of the apo-form GGA1-GAE crystal described above. However, the contact surface areas of the two GGA1-GAE dimmers with the GGA1-hinge peptide (molecules A-B 2,484Å^2 and molecules C-D 2,791 Å^2) are slightly smaller than those of apo-form GGA1-GAE dimers (molecules A-B 2,913 Å^2 and molecules C-D 3,103 Å^2). The structures of two dimers in the GGA1-GAE/hinge complex are identified within r.m.s.d. of 0.6 Å for Cα atoms of the eight β strands. The difference of the contact surface areas between the GGA1-GAE/hinge complex and apo-form GGA1-GAE is caused by sum of the number of hydrophobic interactions and that of hydrogen bonds. In the apo-form GGA1-GAE dimer, the numbers of hydrophobic interaction are 23 and 18 (molecules A-B and C-D) and that of hydrogen bond are 5 and 9 (molecules A-B and C-D). In the case of the complex between GGA1-GAE and the GGA1-hinge peptide, the numbers of hydrophobic interaction are21 (molecules A-B and C-D) and that of hydrogen bond are 4 and 6 (molecules A-B and C-D). These interactions, especially hydrogen bonds, effect on the contact area of GGA1-GAE dimer.

In the GGA1-GAE/hinge complex, the peptides are in extended conformations

and bound on the surface formed by strands β4, β5 and β7 (Fig. 1-6A and B). The tryptophane residue of the peptide is referred as position 0. The N-terminal five residues, (-6)SLDGT(-2), of both peptides (peptide P and Q) are disordered and not visible in the electron density map. The peptide binding mode is essentially the same between the two complexes in the asymmetric unit, although Ser(2) of peptide Q is disordered and could not be observed (Fig. 1-6B). In both complexes, two bulky hydrophobic residues of the peptides at the positions 0 and 3 are accommodated in the two hydrophobic pockets composed of β4 and β7 strands of GGA1-GAE (Fig. 1-6C and D). The side chain of Trp(0) is stuck into the hydrophobic pocket of GGA1-GAE formed by Ala563, Val564 and Pro565 of β4 strand, and aliphatic portions of the side chains of Arg607 and Arg609 of β7 strand. Next, the side chain of Phe(3) is stuck into the hydrophobic pocket formed by Gln561, Ser562 and Ala563 of β4 strand, aliphatic portions of the side chains of Arg609 and Lys611 of β7 strand, and the side chain of Met624 of β8 strand. Additionally, the side chain of Gln(4) makes hydrophobic contacts with Val570 and Leu572 of β5 strand of GGA1-GAE. Except the above common interactions, there are several differences in hydrophobic interactions (Fig. 1-7A and B). The most significant difference is the orientation of the indole ring of Trp(0). The Trp(0) ring of peptide P is approximately perpendicular to that of peptide

Q (Fig. 1-6C and D). In the complex between molecule C and peptide Q, the aromatic ring of peptide Trp(0) stacks with the guanidinium group of Arg609 of GGA1-GAE (Fig. 1-6D). On the other hand, in the complex between molecule A and peptide P, the side chain of Arg609 of GGA1-GAE moves away from the peptide and does not form stacking interaction with Trp(0) (Fig. 1-6C).

In addition to the hydrophobic interactions described above, there are four hydrogen bonds between the main chains of the ligand peptide and β4 strand of GGA1-GAE, resulting in the intermolecular β-sheet formation, in both complexes in the asymmetric unit; the carbonyl of Gly(-1), amide of Asn(1), amide and carbonyl of Gln(4) of the peptide backbone make hydrogen bonds with the amide of Lys566, carbonyl of Val564, carbonyl and amide of Ser562 of the main chain of GGA1-GAE, respectively (Fig. 1-6C, D and 1-7B). In the case of the complex between molecule A and peptide P, additional hydrogen bonds are found between the side chain of Asn(1) and the main chains of Val564 and Pro565 and between the side chain of Ser(5) and the side chain of Gln561 (Fig. 1-6C and 1-7A). In the complex between molecule C and peptide Q, another hydrogen bonds are formed between the main chain of Asn(1) and the main chains of Val564, and between the main chain of Phe(3) and the side chain of Gln561 (Fig. 1-6D and 1-7B).

Crystal structure of complex between GGA1-GAE and an acidic phenylalanine peptide

I also co-crystallized GGA1-GAE with the DDFGDF peptide which is a typical acidic phenylalanine motif of the accessory proteins [D/E][G/A]$_{(0-1)}$F[G/A][D/E]Φ (Duncan and Payne 2003b). Nevertheless, I could observe only poor electron density of the FGDF portion of the peptide at the binding site of GGA1-GAE, which is one of the four molecules in the asymmetric unit (Fig. 1-8A). This may cause of the weak interaction between them due to the lack of additional C-terminal residues to Phe(3) of the peptide. The hydrophobic pocket of GGA1-GAE also formed by Gln561, Ser562, Ala563, Val564 and Pro565 of β4 strand, and aliphatic portions of the side chains of Arg607, Arg609 and Lys611 of β7 strand. There is only one hydrogen bond between the main chain of Gly(1) in the peptide and the main chain of Val564 in GGA1-GAE (Fig. 1-8B). Although two phenylalanine residues are stuck into the two hydrophobic pockets of apo-form GGA1GAE as in the case of the GGA1-hinge peptide, the peptide backbone is slightly shifted away from GGA1-GAE molecules. When I superposed the GAE domains of the GGA1-GAE/DDFGDF and the GGA1-GAE/hinge complexes with Cα atoms of eight β-strands, r.m.s.d. between the DDFGDF peptide and the

GGA1-hinge peptide (peptide P) for four Cα atoms is 1.1 Å (Fig. 1-8C). This suggests that the minimum consensus sequence of the acidic phenylalanine motif is capable of binding to the hydrophobic pockets of GGA1-GAE, however, additional hydrogen bonds which are formed between main chain of the peptide and intermolecular β-sheet of GGA1-GAE may be required for a more stable complex. The four GGA1-GAE molecules in the asymmetric unit form dimers in the crystal through the face-to-face interactions of the β-sheets opposite to the peptide-binding site of GGA1-GAE. However, the orientation between the two GGA1-GAE molecules in the GGA1-GAE/DDFGDF complex is opposite to those in the apo-form GGA1-GAE crystal or the GGA1-GAE/hinge complex. This suggests that the dimerization of GGA1-GAE is due to nonspecific hydrophobic interactions between the β-sheets of GGA1-GAE.

Autoinhibition of GGA1-GAE by the GGA1-hinge region

As described above, I demonstrated that GGA1-GAE interacts with the GGA1-hinge peptide both in solution and in crystal. Thus, in the case of full length GGA1 protein, it would be possible that the GAE domain interacts with the WNSF motif of the hinge region, resulting in autoinhibition of the ligand-binding site of

GGA1-GAE. To further assess this interaction, I carried out fluorescence spectroscopy to monitor possible environmental changes around the tryptophan residue of the WNSF motif upon the autoinhibition. I designed a new construct "GGA1-hinge—GAE" which spans from 350 to 639 residues of GGA1, containing both the hinge region and the GAE domain. To monitor the fluorescence from only Trp382 of the WNSF motif, two other tryptophans (Trp444 and Trp636) were substituted with alanines. These mutations are thought to not interfere with the ligand binding, because both tryptophanes are located apart from the binding site; Trp444 is in the middle of the GGA1-hinge region, and Trp636 is the forth residue from the C-terminus of GGA1-GAE. As a negative control of the autoinhibition, I further introduced a K611Q mutation into the GAE domain of GGA1-hinge—GAE, based on the previous mutational experiment which demonstrated that the corresponding mutation in γ1-ear disrupt the interaction with accessory proteins (Nogi *et al.* 2002). I measured the fluorescence emission spectra of wild-type and K611Q mutant of GGA1-hinge—GAE at the same protein concentration (Fig. 1-9A). The fluorescence intensity of K611Q mutant GGA1-hinge—GAE was reduced and the peak was red-shifted (from 344 nm to 350 nm) compared to wild-type GGA1-hinge—GAE, suggesting that the environment around Trp382 of the K611Q mutant is more hydrophilic than that of the wild-type.

This suggests that the WNSF motif of wild-type GGA1-hinge—GAE construct is shielded by the interaction of GGA1-GAE from the solvent.

Since the interaction between GGA1-GAE and the WNSF motif is similar to that of the GGA-GAE/acidic phenylalanine motif which is previously reported (Collins *et al.* 2003, Miller *et al.* 2003),there may be possible competition between accessory proteins and the GGA1-hinge region at the same binding site of GGA1-GAE. To test this possibility, I measured the fluorescence spectra of GGA1-hinge—GAE with or without the DDFGDF peptide which is used as a model peptide of the consensus acidic phenylalanine motif. A strong quenching of the fluorescence was observed when an excess amount of the peptide was added to wild-type GGA1-hinge—GAE. However, such change was not observed in the K611Q mutant GGA1-hinge—GAE (Fig. 1-9B and C). This suggests that the GGA1-GAE, which bound to the WNSF motif of GGA1-hinge region, dissociates by the addition of the DDFGDF peptide and then the tryptophan residue of the WNSF motif is exposed to the solvent.

Discussion

Comparison with other GAE/acidic phenylalanine motif complexes

In this study, I solved the crystal structure of GGA1-GAE complex with the GGA1-hinge peptide which has the WNSF motif of the GGA1-hinge region. The peptide binding sites are composed of β4, β5, β7 and β8 strands and the loop between β4 and β5 of GGA1-GAE (Fig. 1-10). It has previously reported that two crystal structures which are the complexes between GGA-GAEs and the accessory proteins (Collins *et al.* 2003, Miller *et al.* 2003). Although the WNSF motif deviates from the consensus acidic phenylalanine motif found in the accessory proteins, my structure revealed that its binding mode is essentially the same as the consensus acidic phenylalanine motif. In both cases, two kinds of interactions stabilize the bound peptide in the extended conformation. First, two bulky hydrophobic residues of the peptides at the positions (0) and (3) are accommodated in the two hydrophobic pockets. These hydrophobic pockets are composed of aliphatic portions of the conserved basic residues along with several hydrophobic residues. Second, there are four hydrogen bonds between the main chains of the ligand peptide and β4 strand of GGA1-GAE, resulting in the intermolecular β-sheet formation. In addition to these two interactions, several hydrophobic interactions and hydrogen bonds (occasionally mediated by water

molecules) further stabilize the binding.

Recently, Collins *et al.* reported the structure of GGA1-GAE in complex with the p56 peptide (DDDDE$_{(0)}$GGFEAAETFD) (Collins *et al.* 2003). Interestingly, the side chain of Asp(-1) residue, which is a landmark of the acidic phenylalanine motif, does not make any electrostatic interaction with the basic side chains of GGA1-GAE. Furthermore, electron density corresponds to N-terminus to the Asp(-1), suggesting that the acidic side chains do not make stable contacts with GGA1-GAE. In the case of my complex structure with the GGA1-hinge peptide (SLDGTGW$_{(0)}$NSFQSS), electron density corresponds to N-terminus to Gly(-1) were also invisible. The side chains of Phe(0) and Phe(3) of the p56 peptide are buried in the same hydrophobic pockets of GGA1-GAE which accommodate Trp(0) and Phe(3) of the GGA1-hinge peptide, respectively. The aromatic ring of Phe(0) of the p56 peptide stacks with Arg609 of GGA1-GAE, in a similar orientation to that of Trp(0) of peptide Q in my GGA1-GAE/hinge complex structure. The four hydrogen bonds between the main chain atoms of GGA1-GAE and the p56 peptide are also observed at the equivalent positions in the GGA1-GAE/hinge complex: Asp(-1) to Lys566, Gly(1) to Val564, and two hydrogen bonds from Glu(4) to Ser562.

In the crystal structure of GGA3-GAE in complex with the Rabaptin-5 peptide

(DESDF$_{(0)}$GPLVGADS) (Miller *et al.* 2003), Phe(0) and Leu(3) are accommodated in the hydrophobic pockets of GGA3-GAE as the same manner in the GGA1-GAE/hinge complex, although Leu(3) is only half-buried in the pocket because its side chain is not so bulky compared to that of phenylalanine. The aromatic ring of Phe(0) of Rabaptin-5 peptide stacks with Arg693 of GGA3-GAE, in a similar orientation to that of Trp(0) of peptide Q in my GGA1-GAE/hinge complex structure. The four hydrogen bonds between the Rabaptin-5 peptide and the main chain atoms are also observed at the equivalent positions in the GGA1-GAE/hinge complex: Asp(-1) to Lys650, Gly(1) to Val648 (Val648 was replaced with Ala in their structure) and two hydrogen bonds from Val(4) to Ala646. In the GGA3-GAE/Rabaptin-5 complex, there are additional water-mediated hydrogen bonds. Furthermore, the side chain of Asp(-1) makes a salt bridge with that of conserved Lys650, although the residues which correspond N-terminus to Asp(-1) are invisible in the electron density map. This salt bridge is unique to the GGA3-GAE/Rabaptin-5 structure. This could explain the reason of the tight binding of GGA3-GAE to Rabaptin-5 peptide (K_d:5 μM) (Miller *et al.* 2003) which are stronger than the affinities between GGA1-GAE and the p56 peptide (K_d:68 μM) (Collins *et al.* 2003) and between GGA1-GAE and the WNSF motif (K_d:180 μM).

I also determined the complex structure of GGA1-GAE with the DDF$_{(0)}$GDF

peptide which is a consensus acidic phenylalanine motif of the accessory proteins (Fig. 1-8). I could observe only poor electron density of the DDFGDF peptide, probably due to the low occupancy of the binding site. In this complex, only limited hydrophobic interactions are observed between the two phenylalanines of the DDFGDF peptide and the hydrophobic pockets of GGA1-GAE (Fig. 1-8D). One hydrogen bond is formed between GGA1-GAE and the DDFGDF peptide. These suggest that the intermolecular β-sheet formation between the main chain of Ser562 of GGA1-GAE and the main chain of the peptide residue at position 4, is necessary to stabilize the interaction between GGA1-GAE and the ligand peptide.

Comparison between GGA1-GAE and γ1-ear complexes with the GGA1-hinge peptides

Next I compare the structure of the GGA1-GAE/hinge complex with that of the γ1-ear/GGA1-hinge complex which has been solved recently in our laboratory (Yamada *et al.*2005) (Fig. 1-7). In both complexes, the side chains of Trp(0) and Phe(3) residues are accommodated in the hydrophobic pockets composed of residues in and around the β4 and β7 strands which are well conserved among GGA1-GAE and γ1-ear (Fig. 1-10). In the GGA1-GAE/hinge complex, Trp(0) is surrounded by the side

chains of Ala563, Pro565, Arg607 and Arg609, and Phe(3) is surrounded by the side chains of Gln561, Ala563, Arg609, Lys611 and Met624 (Fig. 1-7A and B). Similarly, in the γ1-ear/GGA1-hinge complex, Trp(0) and Phe(3) are accommodated by the corresponding conserved residues of γ1-ear; Trp(0) is surrounded by the side chains of Ala753, Pro755, Arg793, and Arg795, and Phe(3) is surrounded by the side chains of Gln751, Ala753, Arg795, Lys797 and Leu810 (Fig. 1-7C). There is only one major difference between the two complexes: Arg607 of GGA1-GAE points away from Trp(0) and does not contact with the peptide, whereas the corresponding Arg793 of γ1-ear stacks to the side chain of Trp(0). The orientation of the aromatic ring of Trp(0) bound to γ1-ear is similar to that of Trp(0) of peptide Q bound to GGA1-GAE. Outside of the hydrophobic pockets, there are additional hydrophobic interactions. Among them, the interaction between Gln(4) and Leu572 and that between Ser(5) and Gln561 in the GGA1-GAE/hinge complex are also observed in the γ1-ear/GGA1-hinge complex as interactions between Gln(4) and Leu762 and between Ser(5) and Gln751, respectively.

The four hydrogen bonds between the main chains of the GGA1-GAE/hinge complex are also observed in the γ1-ear/GGA1-hinge complex. In the GGA1-GAE/hinge complex, hydrogen bonds are formed between Gly(-1) and Lys566, between Asn(1) and Val564, and two hydrogen bonds between Gln(4) and Ser562. In

the γ1-ear/GGA1-hinge complex, equivalent four hydrogen bonds are observed: Gly(-1) and Lys756, Asn(1) and Val754, and two hydrogen bonds between Gln(4) amd Ala752. In the γ1-ear/GGA1-hinge complex, there are additional water-mediated hydrogen bonds. Hence, the dissociation constant of the γ1-ear with the WNSF motif (130 μM) is slightly smaller than that of the GGA1-GAE with the WNSF motif (180 μM).

Dimerization of GGA1-GAE

I found that GGA1-GAE forms a dimer in the crystal and in solution. The GGA1-GAE/hinge complex also forms a similar dimer in the crystal. This is reasonable because the dimerization area (β1, β2, β3, β5 and β6 strands, and two loops β2-β3 and β5-β6) is opposite to the peptide binding site (β4, β5 and β7) (Fig. 1-2A and 3). On the contrary γ1-ear does not dimerize in the reported crystal structures (Kent *et al.* 2002, Nogi *et al.* 2002, Yamada *et al.* 2005). The contact area of the other apo-form GGA1-GAE molecules is 2,651 $Å^2$ (Lui *et al.* 2003). This contact area is caused by the crystal packing and has mainly hydrophobic interaction around β2 and β3 strands and in front of β6 strand. These interaction areas are partially common for my GGA1-GAE dimer. But the other GGA1-GAE can't form a dimer because a part of the GGA1-hinge region upstream of GGA1-GAE inhibits the dimerization of GGA1-GAE.

This region has a possibility to cause an inhibition of dimerization or a different shape of GGA1-GAE dimer. The dimer surface was located in the opposite direction of the binding site for accessory proteins and the GGA1-hinge region and GGA1-GAE has two peptide binding sites by dimerization. It is said that GGA1-GAE interacts with several kinds of accessory proteins and in this study I found the interaction with the GGA1-hinge region. The meaning of dimerization is still unknown but I suggest that GGA1 dimerizes the GAE domain to cope with various binding partners.

Autoinhibition of GGA1

The interaction mode between GGA1-GAE and the GGA1-hinge region is similar to that of the previously reported structures of the GGA-GAE/acidic phenylalanine motif complexes (Collins *et al.* 2003, Miller *et al.* 2003), the γ1-ear/acidic phenylalanine motif complex (Yamada *et al.* 2005) and the γ1-ear/GGA1-hinge complex (Yamada *et al.* 2005), suggesting the possible competition between GGA-GAE and γ1-ear for the binding to accessory proteins and the GGA1-hinge region. I therefore measured K_d values of GGA1-GAE with peptides derived from accessory proteins (γ-synergin, EpsinR and Rabaptin-5) and the GGA1-hinge region. These K_d values are comparable suggesting that there is not any dominant peptide in the

competitive interactions. Both GGA1-GAE and γ1-ear interact weakly (~100 μM) with the consensus acidic phenylalanine motif of the accessory proteins and with the WNSF motif of the GGA1-hinge region ranging from 5 to 180 μM of K_d values (Table 1-2). Thus the binding partners of GGA1-GAE and γ1-ear could be interchangeable among accessory proteins and the GGA1-hinge region.

The interaction between GGA1-GAE and the GGA1-hinge region would result in an autoinhibited, i.e., closed form of GGA1 protein. My fluorescent spectroscopy of GGA1-hinge—GAE protein suggested that the tryptophane residue of the WNSF motif in the GGA1-hinge region is in a hydrophobic environment through the interaction with the GGA1-GAE's hydrophobic pocket. An excess amount of the DDFGDF peptide replaces the WNSF motif and pushes it out into the solution, hence the change in the fluorescence signal of the tryptophane. These observations suggest that the GGA1-hinge region and the accessory proteins indeed compete for the interaction with GGA1-GAE. I determined the complex structures of GGA1-GAE with the GGA1 hinge and the DDFGDF peptides and these ligand peptides interact with the same hydrophobic pocket of GGA1-GAE (Figs. 1-6 and 1-8). Mattera *et al.* demonstrated that a recombinant protein fragment having the GGA1-hinge region prior to GGA1-GAE dramatically reduced the affinity to Rabaptin-5 as compared to

GGA1-GAE only (Mattera *et al.* 2003). This corroborates well with the masking of available accessory protein binding site in the hinge—GAE protein due to the autoinhibition.

I could not determine whether the interaction between the hinge region and the GAE domain in GGA1 is intramolecular within a molecule or intermolecular between molecules. The WNSF motif and the GAE domain are 130 residues apart in the amino acid sequence of GGA1. If the GGA1-hinge region is completely extended, the distance between the WNSF motif and the GAE domain could be as long as 490 Å in GGA1. Thus the intramolecular interaction may not be greatly advantageous over the intermolecular interaction, if GGA proteins are relatively abundant.

GGA1 and AP-1 co-localize in the clathrin-coated buds at TGN and cooperate in the packing of the MPRs into clathrin-coated vesicles (Doray *et al.* 2002) presumably through the interaction between the GGA1-hinge region and γ1-ear. It is conceivable that the open form of the GGA1-GAE makes the GGA1-hinge region available for interaction with γ1-ear during the clathrin-coated vesicle assembly. One of the accessory proteins, γ-synergin, co-localizes with both GGA1 and AP-1 on TGN (Page *et al.* 1999, Takatsu *et al.* 2000). It might be possible that the binding of γ-synergin to the GAE domain of the autoinhibited GGA1 relieves the GGA1-hinge region, and allows

the GGA1-hinge region to interact with γ1-ear. On the contrary, the binding of γ-synergin to γ1-ear of the GGA1—AP-1 complex could induce dissociation of GGA1 from AP-1, by competing out the GGA1-hinge region from γ1-ear. In these ways, the autoinhibition of GGA1-GAE may regulate the clathrin-mediated protein transport, through the interactions with various accessory proteins.

References

Bai, H. Doray, B. and Kornfeld, S. (2004) *J. Biol. Chem.* **279**, 17411-17417.

Boman, A.L. Zhang, C. Zhu, X. and Kahn, R.A. (2000) *Mol. Biol. Cell* **11**, 1241-1255.

Brünger, A.T. Adams, P.D. Clore, G.M. DeLano, W.L. Gros, P. Grosse-Kunstleve, R.W. Jiang, J.S. Kuszewski, J. Nilges, M. Pannu, N.S. Read, R.J. Rice, L.M. Simonson, T. and Warren, G.L. (1998) *Acta Crystallogr.* D **54**, 905-921.

Collins, B.M. Praefcke, G.J.K. Robinson, M.S. and Owen, D.J. (2003) *Nature Structural Biol.* **8**, 607-613.

Dell'Angelica, E. C. Puertollano, R. Mullins, C. Aguilar, R. C. Vargas, J. D. Hartnell, L. M. and Bonifacino, J. S. (2000) *J. Cell Biol.* **149**, 81-94.

Doray, B. Ghosh, P. Griffith, J. Geuze, H.J. and Kornfeld, S. (2002) *Science* **297**, 1700-1703.

Duncan, M. C., Costaguta, G., and Payne, G. S. (2003a) *Nat. Cell Biol.* **5**, 77-81.

Duncan, M.C. and Payne, G.S. (2003b) *TRENDS in Cell Biology* **13**, 211-215.

Hirst, J. Lui, W.W. Bright, N.A. Totty, N. Seaman, M.N. and Robinson, M.S. (2000) *J. Cell Biol.* **149**, 67-80.

Hirst, J. Motley, A. Harasaki, K. Peak, Chew. S. Y. Robinson, M. S. (2003) *Mol. Biol. Cell* **14**, 625-641.

Kabsch W. (1976) *Acta. Cryst.* A32 922-923.

Kalthoff, C., Groos, S., Kohl, R., Mahrhold, S. and Ungewickell, E. J. (2002) *Mol. Biol. Cell* **13**, 4060–4073.

Kataoka, M. Hagihara, Y. Mihara, K. and Goto, Y. (1993) *J. Mol. Biol.* **229**, 591-596.

Kent, H.M. McMahon, H.T. Evans, P.R. Benmerah, A. and Owen D.J. (2002) *Structure* **10**, 1139-1148.

Kraulis, P. J. (1991) *J. Appl. Crystallogr.* **24**, 946-950.

Lui, W.W.Y. Collins, B.M. Hirst, J. Motley, A. Millar, C. Schu, P.V. Owen, D. and Robinson, M.S. (2003) *Mol. Biol. Cell* **14**, 2385-2398.

Mattera, R. Arighi, C.N. Lodge, R. Zerial1, M. and Bonifacino, J.S. (2003) *The EMBO Journal* **22**, 78-88.

Merritt 1997 Raster3D

Miller, G.J. Mattera, R. Bonifacino, J.S. and Hurley, J.H. (2003) *Nature Structural Biol.* **8**, 599-606.

Mills, I. G. Praefcke, G. J.K. Vallis, Y. Peter, B. J. Olesen, L. E. Gallop, J.L. Butler, P. J. G. Evans, P. R. and McMahon, H. T. (2003) *J. Cell Biol.* **160**, 213-222.

Mullins, C. and Bonifacino, J. S. (2001) *Mol. Cell Biol.* **21**, 7981-94.

Murshudov, G. N., Vagin, A. A. & Dodson, E. J. (1997) *Acta Crystallogr.* D **53**,

240-255.

Nicholls, A., Sharp, K. A. & Honig, B. (1991) *Proteins Struct. Funct. Gen.* **11**, 281-296.

Nielsen, M.S., Madsen, P., Christensen, E.I., Nykjær, A., Gliemann, J., Kasper, D., Pohlmann, R. and Petersen, C.M. (2001) *EMBO J.* **20**, 2180–2190.

Nogi T, Shiba Y, Kawasaki M, Shiba T, Matsugaki N, Igarashi N, Suzuki M, Kato R, Takatsu H, Nakayama K, and Wakatsuki S. (2002) *Nature Structural Biol.* **9**, 527-531.

Otwinowski 1997 HKL2000

Page, L.J. Sowerby, P.J. Lui, W.W. and Robinson, M.S. (1999) *J. Cell Biol.* **146**, 993-1004.

Poussu, A., Lohi, O. and Lehto, V.-P. (2000) *J. Biol. Chem.* **275**, 7176–7183.

Puertollano, R. Aguilar, R. C. Gorshkova, I. Crouch, R. J. and Bonifacino, J.S. (2001a) *Science* **292**, 1712-1716.

Puertollano, R. Randazzo, P. A. Presley, J. F. Hartnell, L. M. and Bonifacino J.S. (2001b) *Cell* **105**, 93-102.

Roussel, A. and Cambillau, C. *Silicon Graphics Geometry Partners* (Silicon Graphics, Mountain View, CA, 1991).

Takatsu, H. Yoshino, K. and Nakayama, K. (2000) *Biochem Biophys Res Commun.* **271**, 719-725.

Takatsu, H., Katoh, Y., Shiba, Y. and Nakayama, K. (2001) *J. Biol. Chem.* **276**, 28541–28545.

Takatsu, H., Yoshino, K., Toda, K. and Nakayama, K. (2002) *Biochem. J.* **365**, 369–378.

Vagin, A. and Teplyakov, A. (1997) *J. Appl. Cryst.* **30**, 1022-1025.31.

Wallace, A.C. Laskowski, R.A. and Thornton, J.M. (1995) *Prot. Eng.* **8**, 127-134.

Wasiak, S., Legendre-Guillemin, V., Puertollano, R., Blondeau, F., Girard, M., de Heuvel, E., Boismenu, D., Bell, A. W., Bonifacino, J. S. and McPherson, P. S. (2002) *J. Cell Biol.* **158**, 855–862.

Yamada *et al. in preparation.*

Yamada, Y., Inoue, M., Shiba, T., Kawasaki, M., Kato, R., Nakayama, K. and Wakatsuki, S. (2005) *accepted in Acta Cryst. D.*

Zhu, Y., Doray, B., Poussu, A., Lehto, V.-P. and Kornfeld, S. (2001) *Science* **292**, 1716–1718.

Zhdankina, O., Strand, N.L., Redmond, J.M. and Boman, A.L. (2001) *Yeast* **18**, 1–18.

Table 1-1 Crystallographic data

Data set	apo	peptide	
		GGA1-hinge	DDFGDF
Space group	$P2_1$	$P2_12_12_1$	$I222$
Unit cell			
a/*b*/*c* (Å)	47.5/ 88.2/ 67.2	47.9/ 69.1/ 184.8	74.7 / 100.4 / 164.3
$\alpha/\beta/\gamma$ (°)	90/ 96.1/ 90	90/ 90/ 90	90/ 90/ 90
Data collection statistics			
Beam line	PF-AR NW-12	PF-AR NW-12	Spring8-BL38B1
Wavelength (Å)	1	0.978	1
Resolution range (Å)	50- 2.3	50- 2.55	50- 2.65
Outer resolution shell (Å)	(2.36-2.3)	(2.62- 2.55)	(2.72- 2.65)
Observations	85,802	62,150	58,696
Unique reflections	24,237	20,904	18,281
Completeness (%)	98.8 (93.2)	99.7 (99.2)	99.7 (100)
I/σ	12.4 (3.4)	13.1 (3.6)	8.9 (4.9)
R_{sym} (%)	5.6 (29.6)	6.5 (34.5)	8.7 (36.3)
Refinement statistics			
Resolution (Å)	2.3	2.55	2.65
R/R_{free} (%)	22.0/ 26.0	24.1/ 28.7	21.2/25.9
R.m.s. deviation from ideal values			
Bond length (Å)/ Bond angle (°)	0.013/ 1.36	0.017/ 1.78	0.014/1.35
Ramachandran Plot			
Most favoured region (%)	87.0	83.1	89.1
Additionally allowed (%)	12.8	16.5	10.9
Generously allowed (%)	0.2	0.5	0.0
Disallowed region (%)	0.0	0.0	0.0
Average *B*-factors (Å^2)			
All atoms	40.0	44.4	36.2
Protein	42.8	46.8	38.6
Solvent	48.5	37.5	38.5
Peptide P		82.1	55.0
Peptide Q		81.0	

Table 1-2 K_d values of GGA1-GAE and γ1-ear from SPR analyses

peptide	sequence	K_d (μM)	
		GGA1-GAE	γ1-ear*
γ-synergin	$_{666}$LADD**F**GE**F**SLFGE$_{678}$	75	5.1
EpsinR	$_{368}$GNGD**F**GD**W**SAFNQ$_{380}$	110	22
Rabaptin-5	$_{435}$DESD**F**GPLVG$_{444}$	69	61
GGA1-hinge	$_{379}$GTG**W**NS**F**SQ$_{387}$	180	130

Bold letters indicate bulky hydrophobic residues which correspond to positions 0 and 3 of the consensus acidic phenylalanine motif.

*Data of γ1-ear is from Yamada *et al.* in preparation (Yamada *in preparation*).

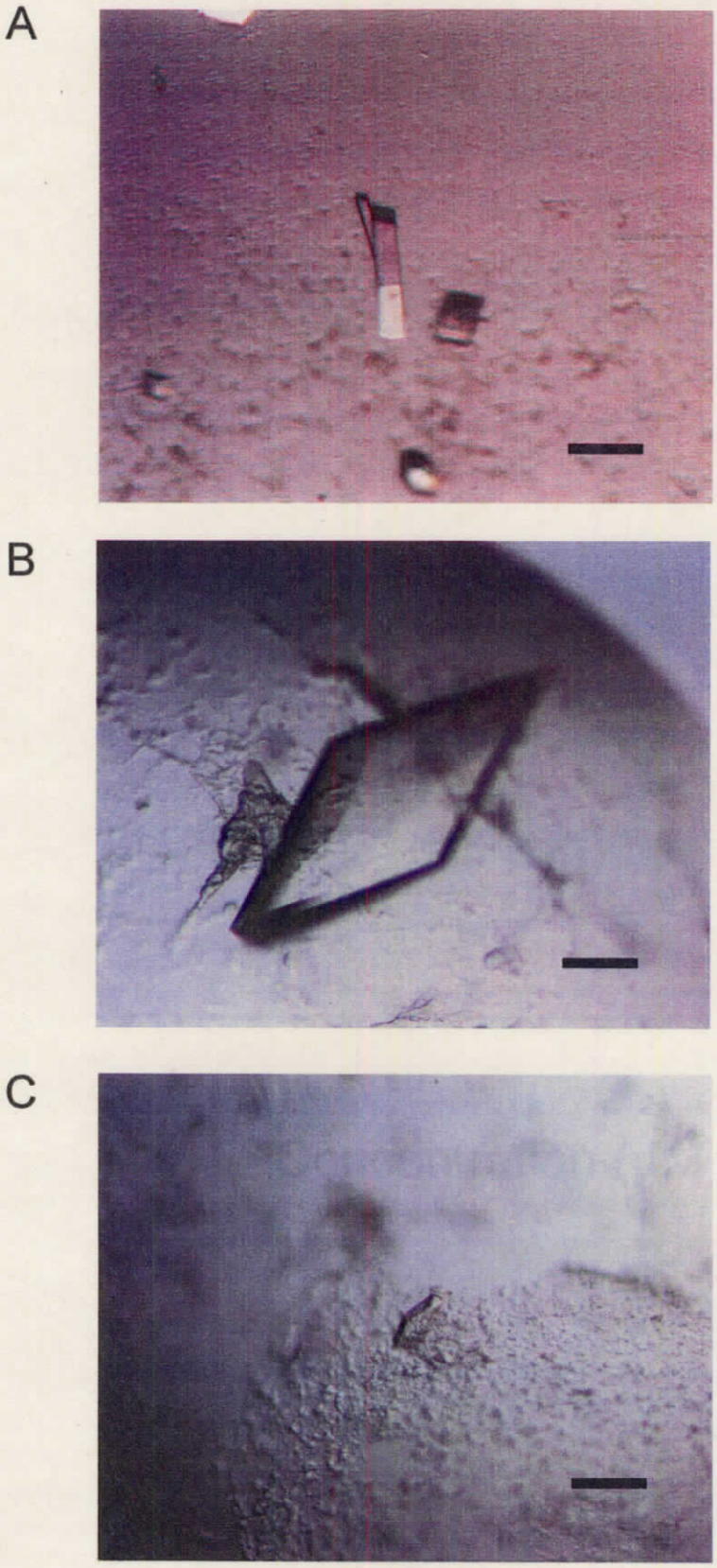

Figure 1-1

Crystals of apo-form GGA1-GAE, the GGA1-GAE/hinge and the GGA1-GAE/DDFGDF complexes. A) Crystal of GGA1-GAE. Its approximate dimensions are 0.05 x 0.05 x 0.2 mm^3. B) Co-crystal of GGA1-GAE with the GGA1 hinge peptide. Its approximate dimensions are 0.3 x 0.3 x 0.6 mm^3. C) Co-crystal of GGA1-GAE with the DDFGDF peptide. Its approximate dimensions are 0.05 x 0.05 x 0.1 mm^3. Bar shows 0.1 mm.

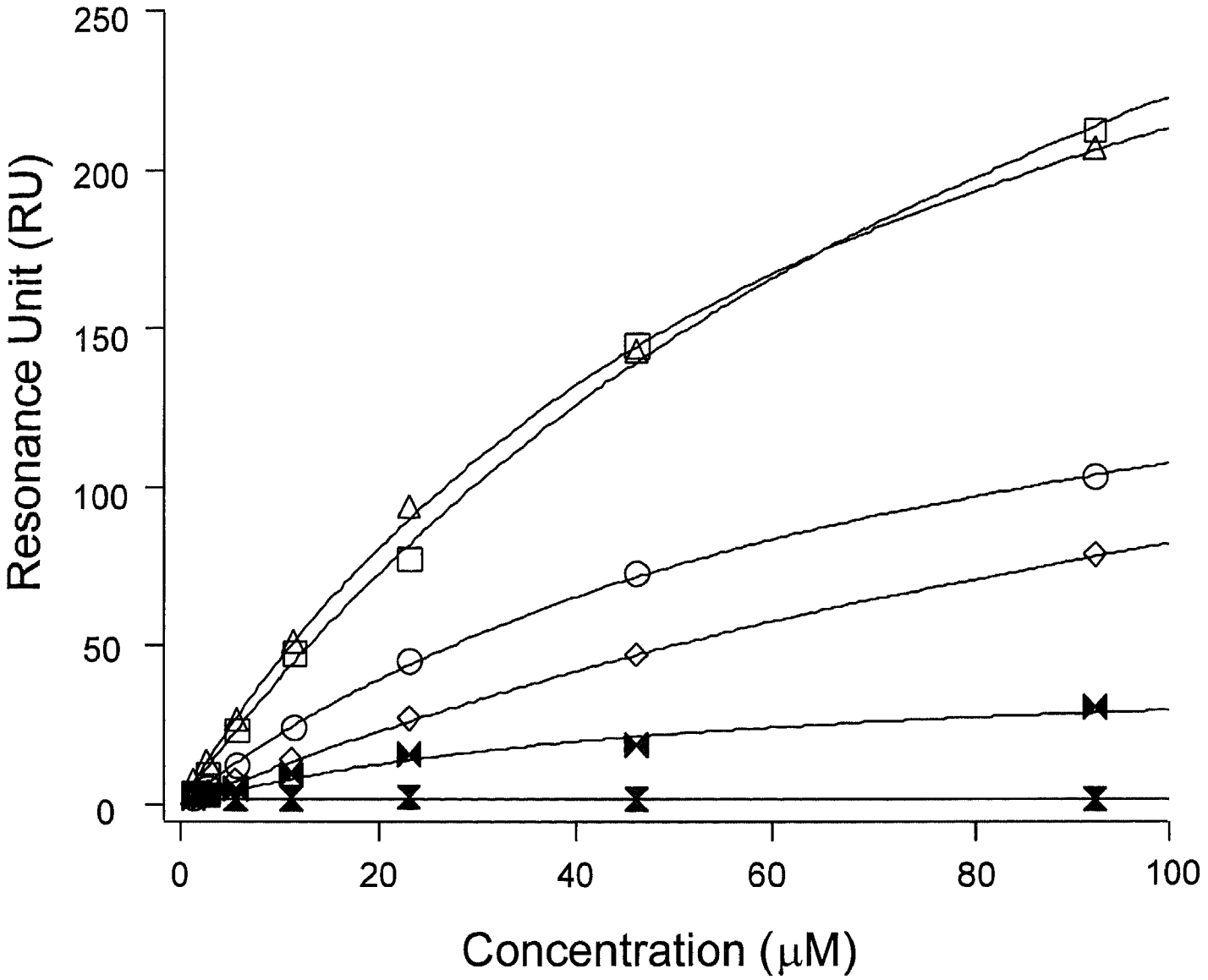

Figure 1-2
SPR signals of the steady state binding of GGA1-GAE to the immobilized GST-fusions of ligand peptides are plotted against GGA1-GAE concentrations. Circle (○), square (□), triangle (△) and diamond (◇) indicate the peptides for γ-synergin, EpsinR, Rabaptin-5 and GGA1-hinge, respectively. Filled symbols (⋈, ⧗) are those for W382A and F385A mutants of the GGA1-hinge peptide. The continuous lines are the fitted curves.

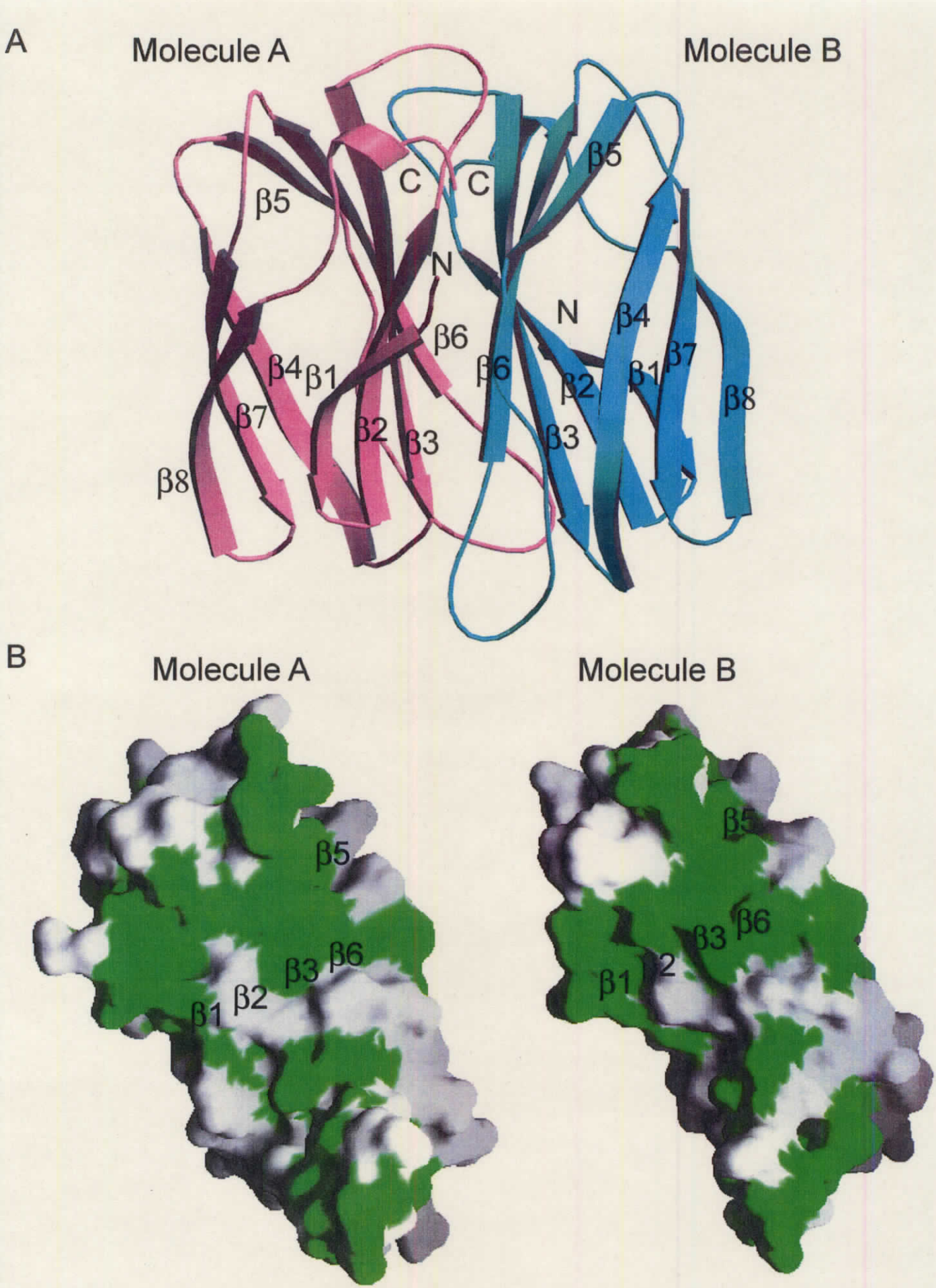

Figure 1-3
Dimerization of GGA1-GAE in crystal. (A) Overall structure of GGA1-GAE dimer molecule. GGA1-GAEs are shown by ribbon models. A pseudo two-fold axis exists between the two molecules. (B) Open book representation of dimerization surfaces of GGA1-GAEs. The hydrophobic residues are colored green.

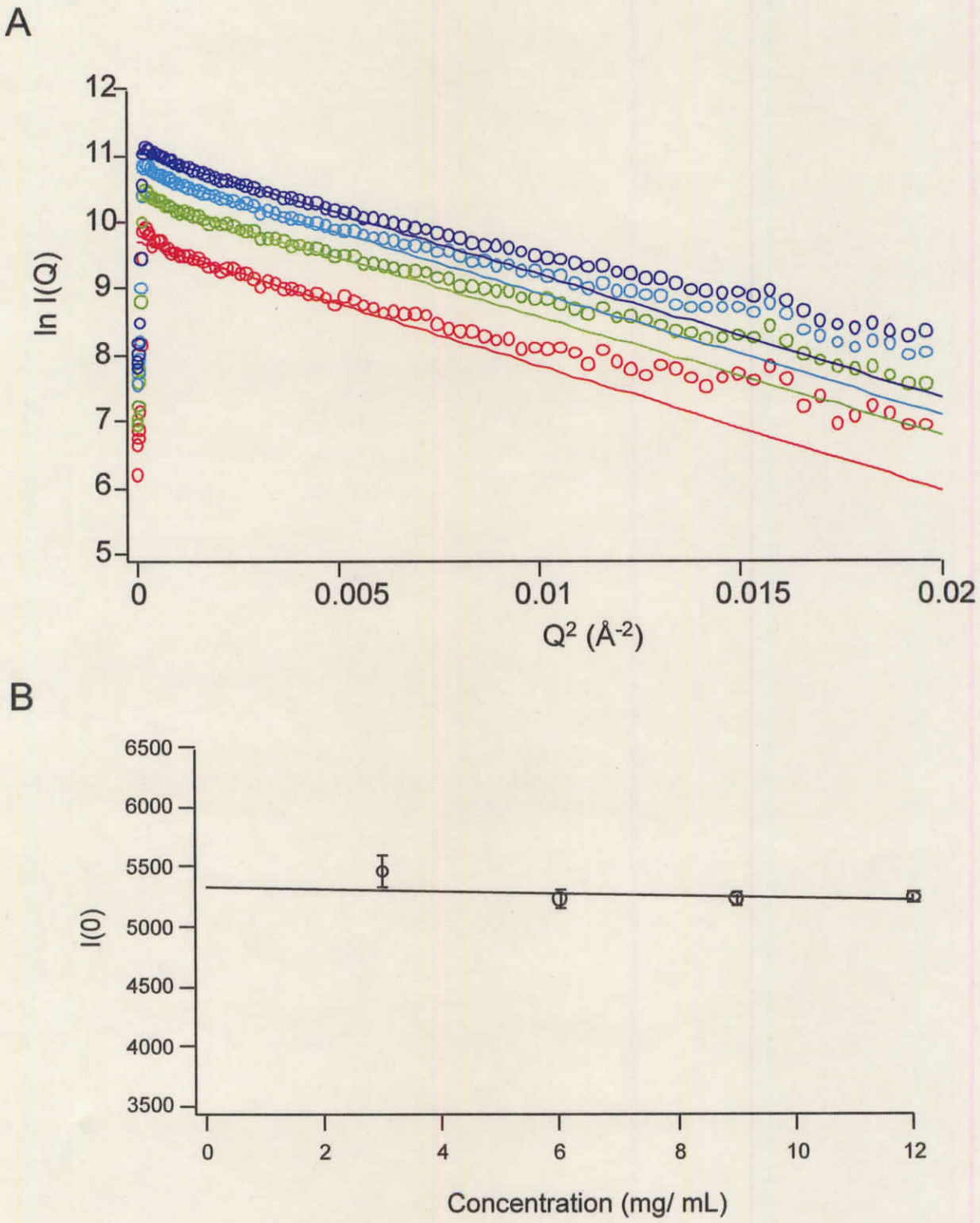

Figure 1-4
SAXS profiles of GGA1-GAE. A) Guinier plots of GGA1-GAE at various protein concentration. Red circles show 3 mg/ mL of GGA1-GAE, green ones show 6 mg/ mL, cyan ones are 9 mg/ mL and blue ones are 12 mg/ mL, respectively. Continuous lines indicate the fitting lines by Guinier regions. B) The plot of scattering intensity at origin vs. concentration of GGA1-GAE.

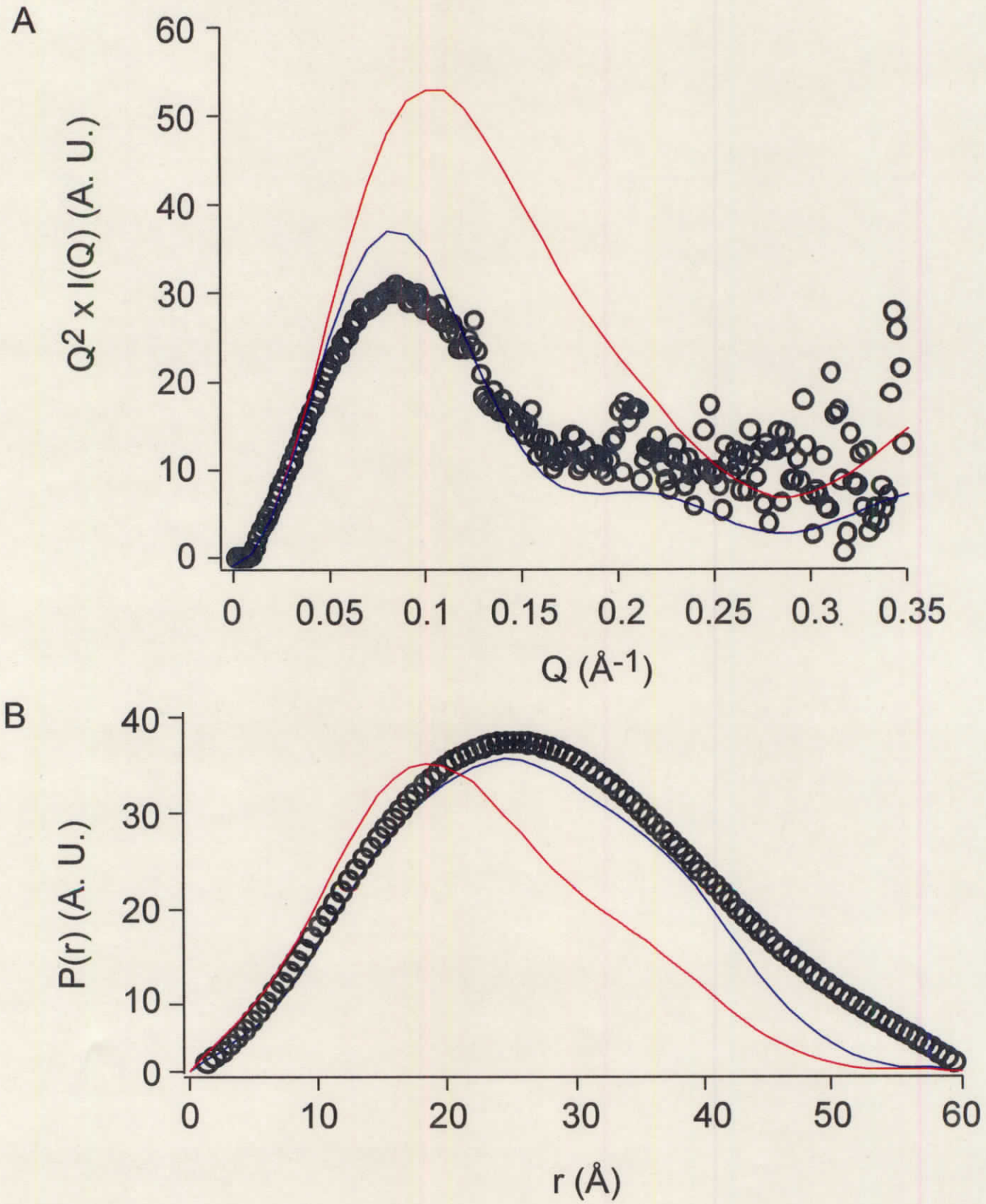

Figure 1-5
Scattering profiles of GGA1-GAEs calculated from SAXS measurement and crystal structures A) Comparison of Kratky plots of GGA1-GAE from SAXS experiment and from the crystal structures. Black circles were plotted from the experiment of 12 mg/mL GGA1-GAE. Red and blue lines were calculated from monomer and dimer molecules of GGA1-GAE in the crystal, respectively. B) Comparison of P(r) functions. Black circles were plotted from SAXS data of 12 mg/mL GGA1-GAE. Blue and red lines were calculated from monomer and dimer molecules of GGA1-GAE in the crystal, respectively. A. U. means Arbitrary Unit.

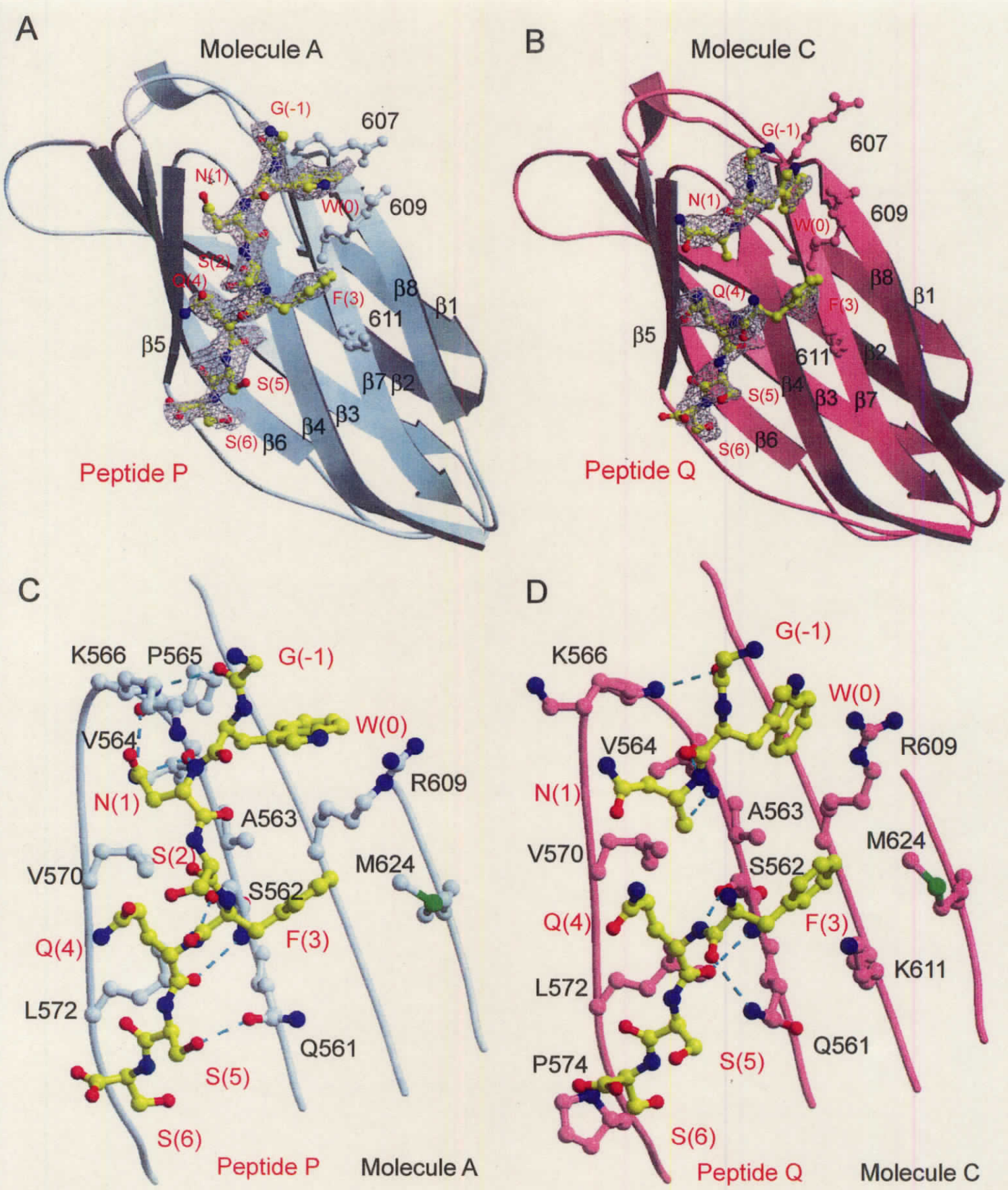

Figure 1-6

Structures of the GGA1-GAE/hinge complexes. (A) & (B) GGA1-GAE with the GGA1-hinge peptides. GGA1-GAE and the peptide are shown by ribbon models and ball-and-stick models, respectively. Electron density contoured at 2.0 σ is shown for binding peptides in Fo-Fc map. (C) & (D) Detailed view of the interaction between GGA1-GAE and the GGA1-hinge peptide. Main chains of GGA1-GAE are shown as coil model and side chains of the proteins and the peptides involved in the interaction are shown by ball-and-sticks. The black letters indicate the residues of GGA1-GAE and the red letters are residues of the peptide. Cyan dot lines show hydrogen bonds.

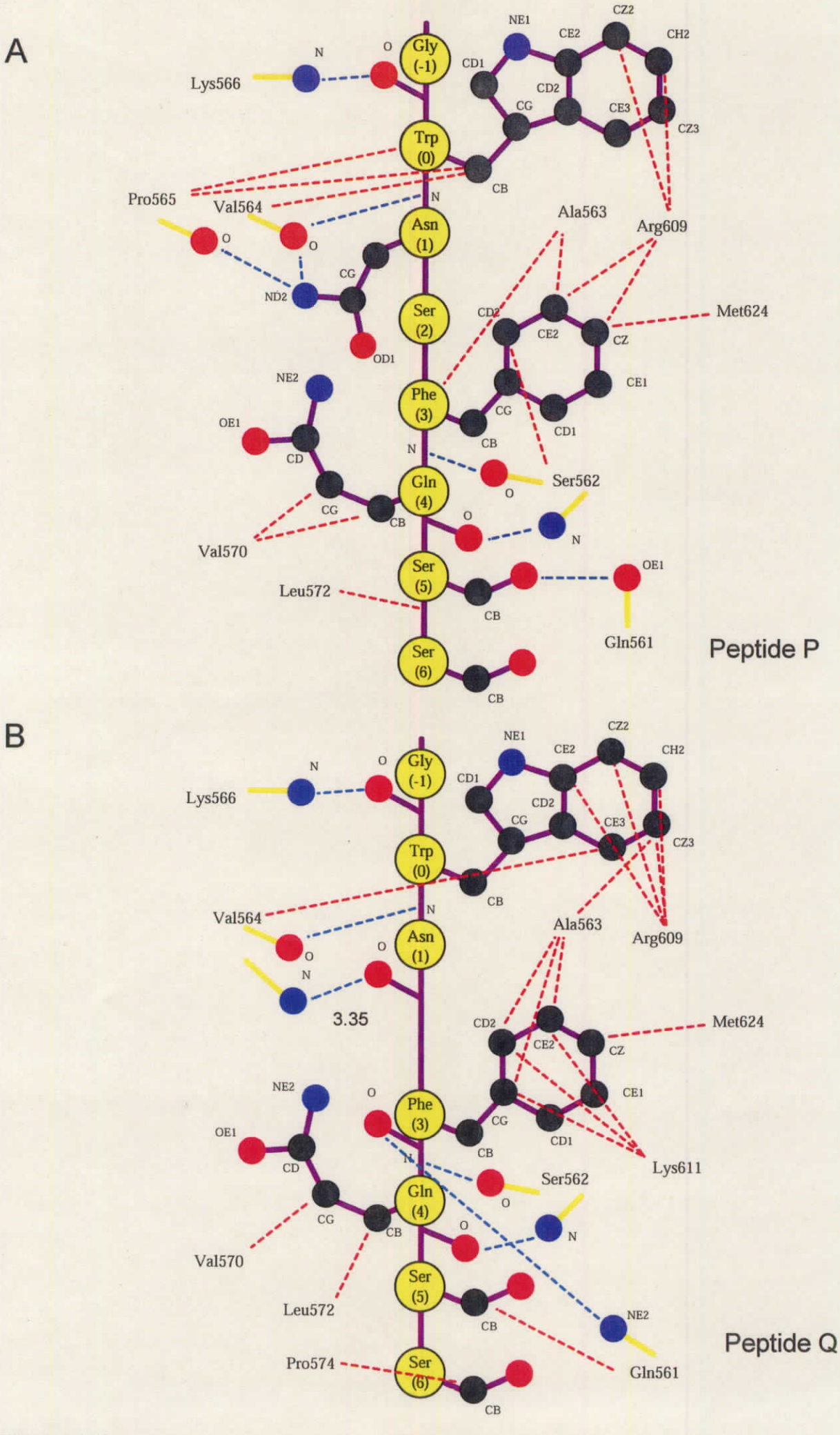
A
Lys566
Gly (-1)
Trp (0)
Pro565
Val564
Asn (1)
Ser (2)
Phe (3)
Gln (4)
Ser (5)
Ser (6)
Ala563
Arg609
Met624
Ser562
Val570
Leu572
Gln561
Peptide P
B
Lys566
Gly (-1)
Trp (0)
Val564
Asn (1)
3.35
Ala563
Arg609
Met624
Phe (3)
Lys611
Ser562
Gln (4)
Val570
Leu572
Ser (5)
Pro574
Ser (6)
Gln561
Peptide Q

Figure 1-7

C

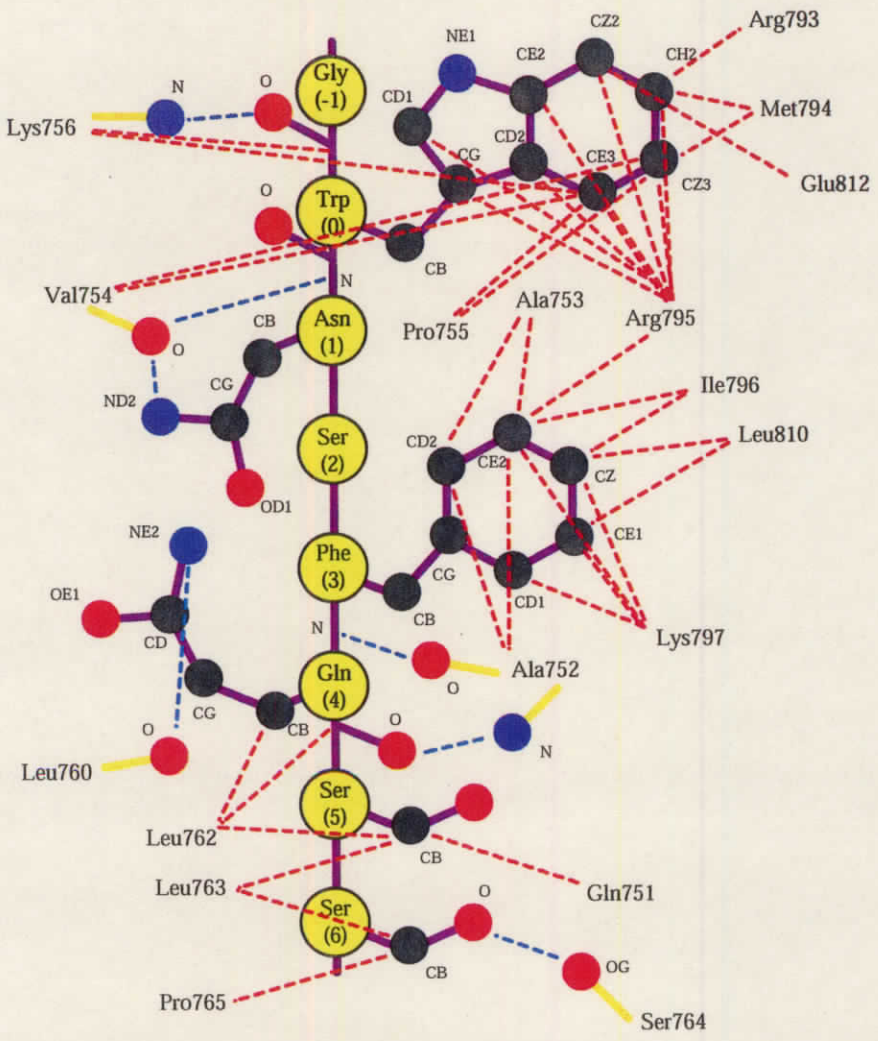

Figure 1-7 (continued)
Schematic representation of the interaction between GGA1-GAE and the GGA1-hinge peptide. Red and blue broken lines indicate the hydrophobic interactions and hydrogen bonds, respectively. The GGA1 -hinge peptide and the nitrogen and oxygen atoms for hydrogen bonds are shown by ball-and-stick model. (A) Interaction between GGA1-GAE (molecule A) and the GGA1-hinge peptide (peptide P). (B) Interaction between GGA1-GAE (molecule C) with the GGA1-hinge peptide (peptide Q). (C) Interaction between γ1-ear and the GGA1-hinge peptide.

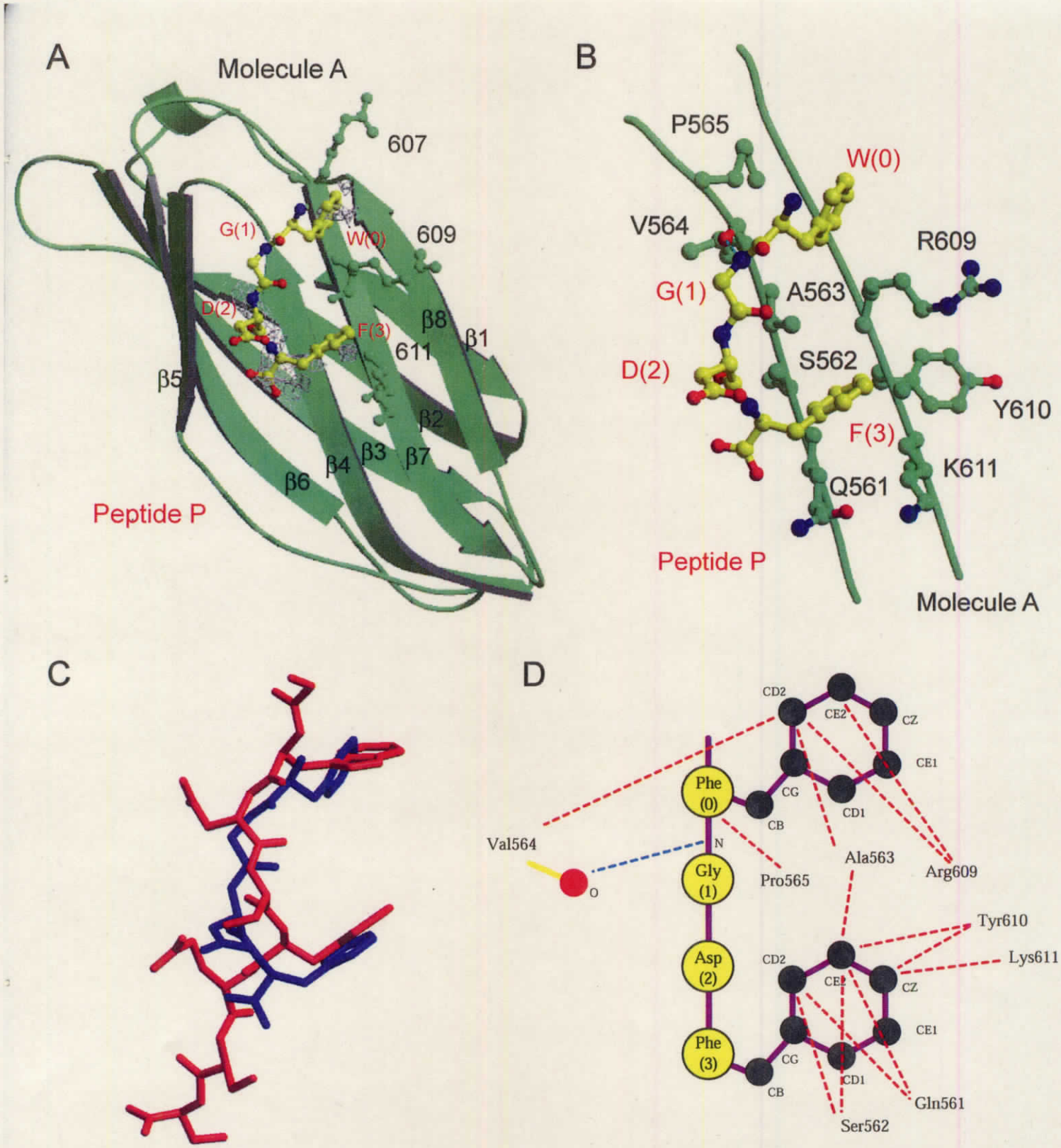

Figure 1-8

Structure of the GGA1-GAE/DDFGDF complex. (A) GGA1-GAE and the DDFGDF peptide are shown by ribbon models and ball-and-stick models, respectively. Electron density contoured at 1.5 σ is shown for binding peptides in Fo-Fc map. (B) Detailed view of the interaction between GGA1-GAE and the DDFGDF peptide. Main chains of GGA1-GAE are shown as coil model and side chains of the protein and the peptides involved in the interaction are shown by ball-and-sticks. The black letters indicate the residues of GGA1-GAE and the red letters are residues of the peptide. Cyan dot line shows hydrogen bond. (C) Superposition of ligand peptides. All peptides are shown by bonds model. Blue is the DDFGDF peptide. Red is the GGA1-hinge peptide (molecules P). (D) Schematic representation of the interaction between GGA1-GAE and the DDFGDF peptide. Red and blue dotted lines indicate the hydrophobic interactions and hydrogen bonds, respectively. DDFGDF peptide and the nitrogen and oxygen atoms for hydrogen bonds are shown by ball-and-stick model.

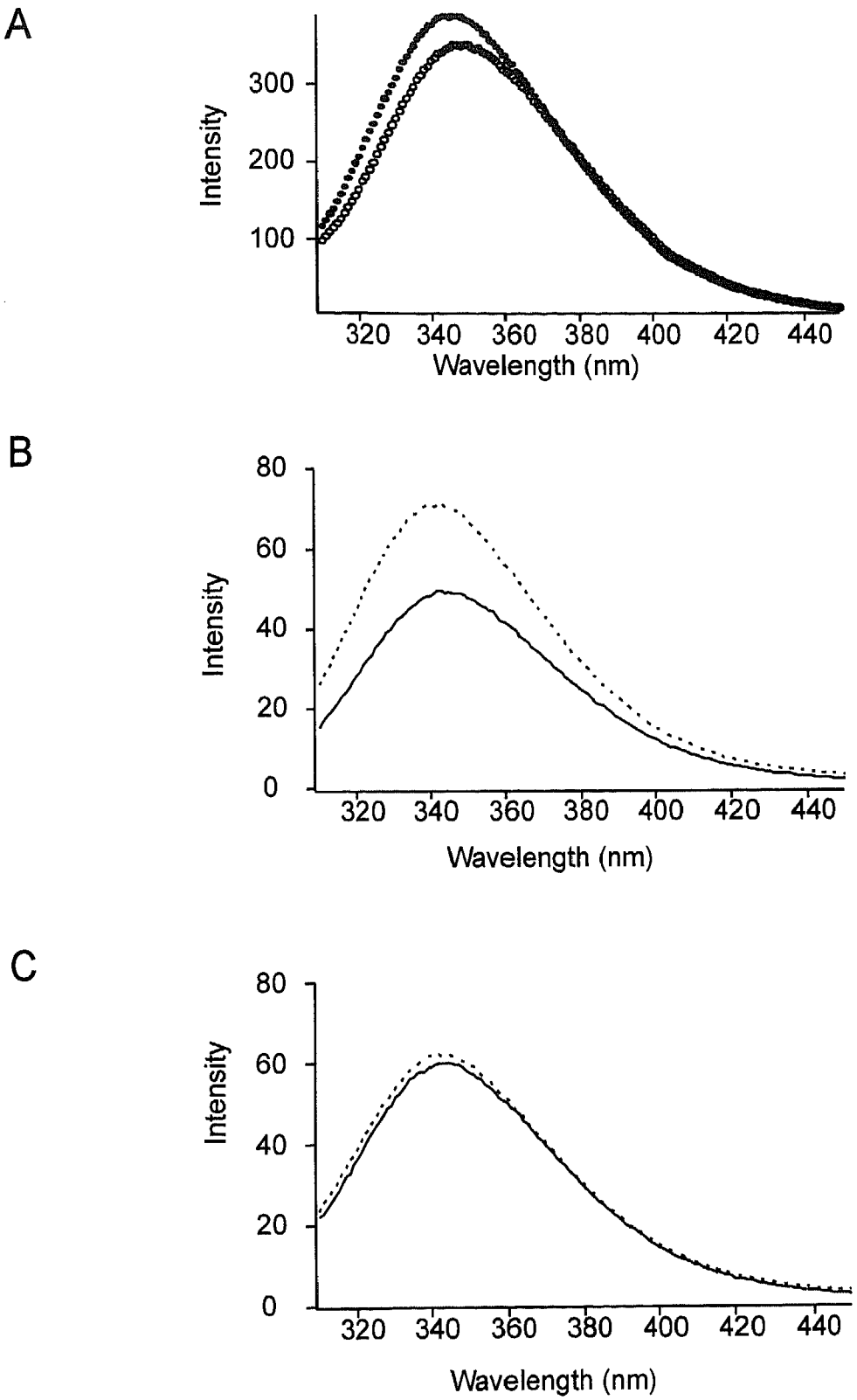

Figure 1-9
Fluorescence spectra of GGA1-hinge—GAE (A) Comparison of the wild type and the K611Q mutant of GGA1-hinge—GAE; filled and open circles show the fluorescence spectra of the wild-type and the mutant, respectively. Spectra were measured at concentrations of 20 μM of wild-type and K611Q mutant GGA1-hinge—GAE. Fluorescence spectra of wild-type (B) and K611Q mutant GGA1-hinge—GAEs (C) with and without the DDFGDF peptide are shown. Solid lines: the fluorescence spectra with the DDFGDF peptide; Dotted lines: a summation of the individual spectra of GGA1-hinge—GAEs and that of the DDFGDF peptide. Spectra were measured for solutions containing 2 μM of both GGA1-hinge—GAEs and/or 1 mM DDFGDF peptide.

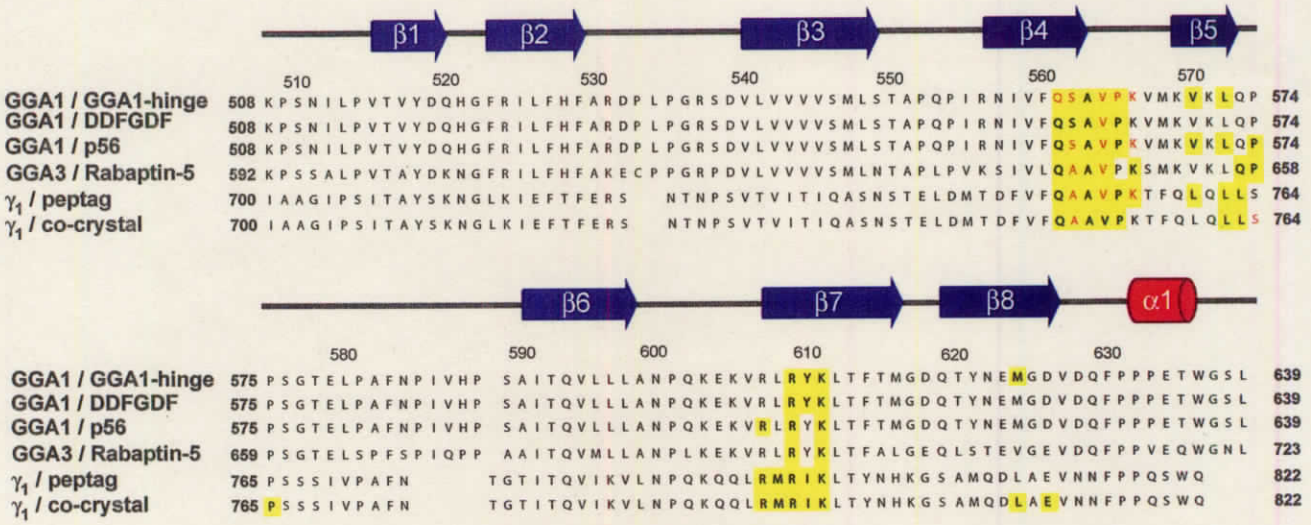

Figure 1-10

The sequence alignment of the complex structures of GGA-GAEs and γ1-ear with peptides. Yellow boxes and red characters show residues of the proteins forming the hydrophobic and hydrophilic interactions with the cognate peptides, respectively. Blue allows show the β-strands of GGA1-GAE.

Appendix: SKD1

Summary

SKD1 (suppressor of K^+ transport growth defect 1) belongs to the AAA (ATPases associated with diverse cellular activities) type ATPase family. AAA proteins participate in the various cellular mechanisms, protein degradation, membrane fusion, DNA replication and so on. It is thought that AAA proteins form oligomeric rings to carry out their various functions. SKD1 is required for vesicle formation in the MVB sorting between endosome and lysosome. But the detail function and mechanism of SKD1 are unknown. To reveal the relationship between the function and the assembly structure, I tried to determine the crystal structure of SKD1.

I succeeded in the expression and purification of recombinant mouse SKD1 in *E. coli*. During the gel-filtration of the purification step, I found that SKD1 was two assemble conditions in solution. And I succeeded in the crystallization of SKD1. I improved the resolution of the diffraction using by a nucleotide soaking method and collected the dataset up to 4 Å. Crystallographic analysis showed that SKD1 forms an oligomer in crystal. These observations suggest that SKD1 forms a mixture of monomer and oligomer to function the vesicle formation in the MVB sorting.

Introduction

SKD1 (suppressor of K^+ transport growth defect 1) belongs to the AAA (ATPases associated with diverse cellular activities) type ATPase family. At the first time, mouse *SKD1* gene was identified as the suppressor gene of the growth deficiency of a potassium transport mutant in *Saccharomyces cerevisiae* (*S. cerevisiae*) (Pèrier *et al.* 1994). After that, it was found that *SKD1* gene was homologue of yeast *vps4* (vacuolar protein sorting) gene which is one of classE *vps* genes (Scheuring *et al.* 1999). *vps* mutants possess vacuolar morphologies that differed significantly from wild-type vacuoles and classE *vps* mutants possess an exaggerated form of a pre-vacuolar endosome-like compartment (Raymond *et al.* 1992). Vps4 also belongs to the protein family of AAA-type ATPases and it is said that Vps4 function is required for efficient transport out of the pre-vacuolar endosome (Babst *et al.* 1997). The nucleotide-free and ADP-bound forms of Vps4 existed as a dimer whereas Vps4 dimers assembled into a decameric complex in the ATP-locked state (Babst *et al.* 1998). It is suggested that Vps4 ATPase catalyzes the release of endosomal membrane-associated classE Vps protein complexes required for normal morphology and sorting activity of the endosome. In the case of SKD1, when dominant negative mutant SKD1 (E235Q) which looses the ATPase activity was overexpressed, carrier proteins couldn't be

transported from early endosome to lysosome or recycling endosome and was accumulated in early endosome (Yoshimori *et al.* 2000). It has also been reported that wild-type SKD1 was cytosolic, whereas mutant SKD1 was localized to endosomal membranes and blocked the cholesterol sorting (Bishop and Woodman 2000). These results show that SKD1 regulates morphology of endosomes and endosomal membrane transport and that the function of SKD1 is equivalent to that of Vps4.

Recently, it is proposed the model for the MVB (multivesicular body) sorting by the classE Vps protein machinery in *S. cerevisiae* (Bast *et al.* 2002). In this model, first ESCRT (endosomal sorting complex required for transport) I complex recognizes ubiquitinated endosomal cargo protein. Second ESCRT II and III complexes assemble and interact with ESCRT I for cargo protein sorting and vesicle formation. Finally Vps4 helps to form vesicles including cargo proteins and disassembles the MVB sorting components (ESCRT I/II/III). In the mammalian cell, MVB sorting is not still constructed but many ESCRT homologue proteins were found and related to each other and also Vps4B alias SKD1 interacted with human ESCRT III (von Schwedler *et al.* 2003). The AAA proteins carry out a wide variety of cellular functions; protein degradation, membrane fusion, assembly and disassembly of protein-protein and protein-nucleic acid complexes, DNA replication and recombination, and transcriptional

activation. AAA proteins form the ring-shape oligomer and most of them form hexameric rings. Oligomerization of AAA proteins is required for their functions. Vps4 forms dimer and decameric complex but it is unclear what assembly condition does SKD1 form in the cell and how SKD1 functions in MVB sorting. And recent studies show that most of infectious HIV-1 (human immunodeficiency virus type 1) is assembled in late endosome in primary macrophages (Pelchen-Matthews *et al.* 2003) and that the p6 region of HIV-1 interacted with human ESCRT III through AIP1/ALEX (Strack *et al.* 2003). Dominant negative SKD1 E235Q mutant experiment shows that SKD1 also related to the release of HIV-1 budding (von Schwedler *et al.* 2003). Investigation of MVB sorting system, especially SKD1, causes to understand not only the endosomal transport but also invasion pathway of HIV-1.

Experimental procedures

Expression and purification of SKD1

A DNA fragment for mouse SKD1 was cloned into the pProEXHTb plasmid (Invitrogen) as 6×His tag protein and expressed in *E. coli* BL21 (DE3) pLysE cells. The cells were disrupted by sonication on ice and centrifuged for 90 min with 18,000 rpm. The supernatant was applied onto a His-tag affinity column of Ni-NTA (QIAGEN) and was eluted by 500 mM imidazole in 20 mM Tris-HCl (pH 8.0) and 5 mM β-mercaptoethanol. Eluted His-tag SKD1 purified by an anion exchange column of HiPrep DEAE FF (Amersham Pharmacia Biotech) with a linear gradient of 0-1 M NaCl in 20 mM Tris-HCl (pH 8.0) and 5 mM β-mercaptoethanol.

The His-tagged protein was cleaved by TEV protease (Invitrogen) at 5 units/mL for 24 hrs at 295 K. The cleaved SKD1 was further purified by Superdex 200 size-exclusion column chromatography in 5 mM β-mercaptoethanol and 20 mM Tris-HCl (pH 8.0). The purified protein was finally obtained as a single band, stained with Coomassie brilliant blue, in SDS polyacrylamide gel electrophoresis.

Crystallization of SKD1 and data collection

The purified protein in 20 mM Tris-HCl buffer pH 8.0 containing 5 mM

β-mercaptoethanol was concentrated to about 10 mg/mL in a Centriprep YM-10 concentrator (Amicon) at 277K. All crystallization experiments were carried out with the hanging-drop vapor diffusion method using VDX Plate Greased (Hampton Research). Preliminary crystallization conditions were established using Hampton Research Crystal Screen Kit 1, 2, MembFac screen, PEG/ION screen, Natrix screen and Emerald BioStructures Wizard I, II, Cryo I, II. Crystals of SKD1 (0.05 x 0.05 x 0.35 mm^3) were obtained in a buffer solution containing 10 mg ml^{-1} protein, 5 % (wt./vol.) PEG3350 and 100 mM MES (pH 6.0) after three days at 293 K (Fig. 2-1A).

The data set of SKD1 crystal was collected at AR-NW12 of Photon Factory (Tsukuba, Japan) on the Quantum 210 CCD system. The wavelength was set to 1 Å with a crystal-to-detector distance of 300 mm and an exposure time of 3 sec per degree of oscillation. . All data sets were collected under cryogenic conditions with crystals soaked in a cryoprotectant solution containing 10 % (wt./vol.) glycerol and cooled at 100 K in a nitrogen gas stream. X-ray diffraction data were collected up to 8 Å resolution. To improve the X-ray diffraction of SKD1, I soaked the crystals into soaking solutions containing 1mM ADP, ATP and some adenosine nucleotide analogues (AMPPNP and ATPγS), 7.5 % (wt./vol.) PEG3350, 100 mM MES (pH 6.0) and 15 % glycerol for 5 min to 1 hr. I succeeded in the improvement of diffraction images after

the soaking of AMPPNP for 1 hr. X-ray diffraction data were collected up to 4 Å resolution The data were processed, integrated and scaled with the program HKL2000 (Otwinowski 1997). The crystal of SKD1 belongs to hexagonal with unit-cell dimensions of $a=b=76.0$ Å, $c=131.7$ Å, $\gamma=120°$. The presence of SKD1 molecule, with a molecular weight of 49.4 kDa, in the asymmetric unit gives a crystal volume per protein mass V_M of 2.27 $Å^3$/Da and a solvent content of 45.9 %, which lies within the ranges usually found for protein crystals (Matthews 1968). The crystallographic data were shown in Table 2-1.

Results and discussion

The assembly condition of SKD1 in solution

I succeeded in the expression and purification of recombinant SKD1. During purification, I found that SKD1 solution separated to two peaks in gel-filtration (Fig. 2-2). Maximum fractionation ability of Superdex200 is upto 200 kDa and I roughly calculated the molecular weights of two SKD1 peaks from the elution to be over 200 kDa and about 50 kDa, respectively. The latter coincides well with the molecular weight of SKD1 from its amino acid sequence. During the purification, SKD1 sample tends to increase the ratio of oligomer. These observations suggest that SKD1 existed monomer and oligomer in solution under some equilibrium condition.

Crystallization of SKD1

I succeeded in I tried to determine and refine the crystal structure of SKD1 by the molecular replacement method with the program MOLREP (Vagin *et al.* 1997). Several AAA proteins were determined their crystal structures (Ogura and Wilkinson 2001). One of AAA proteins, p97, has two AAA motifs of D1 and D2 domains in its amino acid sequence and functions in membrane fusion and proteolysis (Zhang *et al.* 2000). I used the structure of p97 D1 domain (PDB accession number: 1E32) as a

search model of molecular replacement method. I modified the search model as the alanine model of p97 D1 domain (195-426) which is α/β subdomain and α subdomain of AAA core motif. After Molrep running, R-factor of SKD1 first model was 52.9%. This model was refined using CNS (Brünger *et al.* 1998) for the resolution range 50-4.0 Å. First CNS running refined the model as 45.9 % of R-factor and 52.8% of freeR. The refinement of SKD1 structure was not improved. Some secondary structures of SKD1 rough model were matched to the electron density map in the first CNS running SKD1 model (Fig. 2-3). This rough model structure of SKD1 seemed to interact with each neighbor molecules and to be located as spiral rosary in crystal (Fig.2-4). This observation may suggest that SKD1 molecule forms oligomer. These results suggest that SKD1 have two assembly conditions, monomer and oligomer to regulate it's own function as same as some AAA proteins.

In this study, I succeeded in the crystallization of SKD1 protein and in the data collection of SKD1 crystal up to 4 Å resolution. This resolution is enough for crystal structure analysis but I have not succeeded in the determination of the crystal structure of SKD1 yet. I could not determine whether SKD1 oligomer was composed of hexamer like other AAA proteins or not, whereas I demonstrated the possibility of the SKD1 oligomeric conformation. I would like to improve the crystal structural analysis

of SKD1 to reveal the relation between the function and the structure.

References

Babst, M., Sato, T. K., Banta, L. M. and Emr, S. D. (1997) *The EMBO J.* **16**, 1820-1831.

Babst, M., Wendland, B., Estepa E. J. and Emr, S. D. (1998) *The EMBO J.* **17**, 2982–2993.

Babst, M., Katzmann, D.J., Estepa-Sabal, E.J., Meerloo, T. and Emr, S.D. (2002) *Dev. Cell* **3**,271-282.

Bishop, N. and Woodman, P. (2000) *Mol. Biol. Cell* **11**, 227–239.

Brünger, A.T. Adams, P.D. Clore, G.M. DeLano, W.L. Gros, P. Grosse-Kunstleve, R.W. Jiang, J.S. Kuszewski, J. Nilges, M. Pannu, N.S. Read, R.J. Rice, L.M. Simonson, T. and Warren, G.L. (1998) *Acta Crystallogr.* D **54**, 905-921.

Matthews, B. W. (1968) *J. Mol. Biol.* **33**, 491-497.

Otwinowski 1997 HKL2000

Ogura, T. and Wilkinson, A. J. (2001) *Gene to Cells* **6**, 575-597.

Pelchen-Matthews, A., Kramer, B. and Marsh M. (2003) *J. Cell Biol.* **162**, 443-455

Strack, B., Calistri, A., Craig, S., Popova, E. and Göttlinger, H. G. (2003) *Cell* **114**, 689-699.

Pèrier, F., Coulter, K. L., Liang, H., Radeke, C. M., Gaber, R. F., Vandenberg, C. A.

(1994) *FEBS Letters* **351**, 286-290.

Raymond, C. K., Howald-Stevenson, I., Vater, C. A. and Stevens, T. H. (1992) *Mol. Biol. Cell* **3**, 1389-1402.

Scheuring, S., Bodor, O., Rohricht, R.A., Muller, S., Beyer, A. and Kohrer, K. (1999) *Gene* **234**, 149-159.

Vagin, A. and Teplyakov, A. (1997) *J. Appl. Cryst.* **30**, 1022-1025.31.

von Schwedler, U. K., Stuchell, M., Muller, B., Ward, D.M., Chung, H.Y., Morita, E., Wang, H. E., Davis, T., He, G.P., Cimbora, D. M., Scott, A., Kräusslich, H.G., Kaplan, J., Morham, S.G. and Sundquist, W.I. (2003) *Cell* **114**, 701-713.

Yoshimori, T., Yamagata, F., Yamamoto, A., Mizushima, N., Kabeya, Y., Atsuki Nara, A., Ishido, M., Ohashi, M., Ohsumi, M. and Ohsumi, Y. (2000) *Mol. Biol. Cell* **11**, 747–763.

Zhang, X., Shaw, A., Bates, P.A., Newman, R.H., Gowen, B., Orlova, E., Gorman, M.A., Kondo, H., Dokurno, P., Lally, J., Leonard, G., Meyer, H., van Heel, M. and Freemont, P. S. (2000) *Molecular Cell* **6**, 1473–1484.

Table 2-1 Crystallographic data

Data set	SKD1
Space group	$P6_5$
Unit cell	
a/*b*/*c* (Å)	76.0/ 76.0/ 131.7
$\alpha/\beta/\gamma$ (°)	90/ 90/ 120
Data collection statistics	
Beam line	PF-AR NW-12
Wavelength (Å)	1
Resolution range (Å)	50- 4
Outer resolution shell (Å)	(4.14-4.00)
Observations	40357
Unique reflections	3678
Completeness (%)	99.9 (100)
I/σ	8.2 (5.92)
R_{sym} (%)	10.3 (47.1)

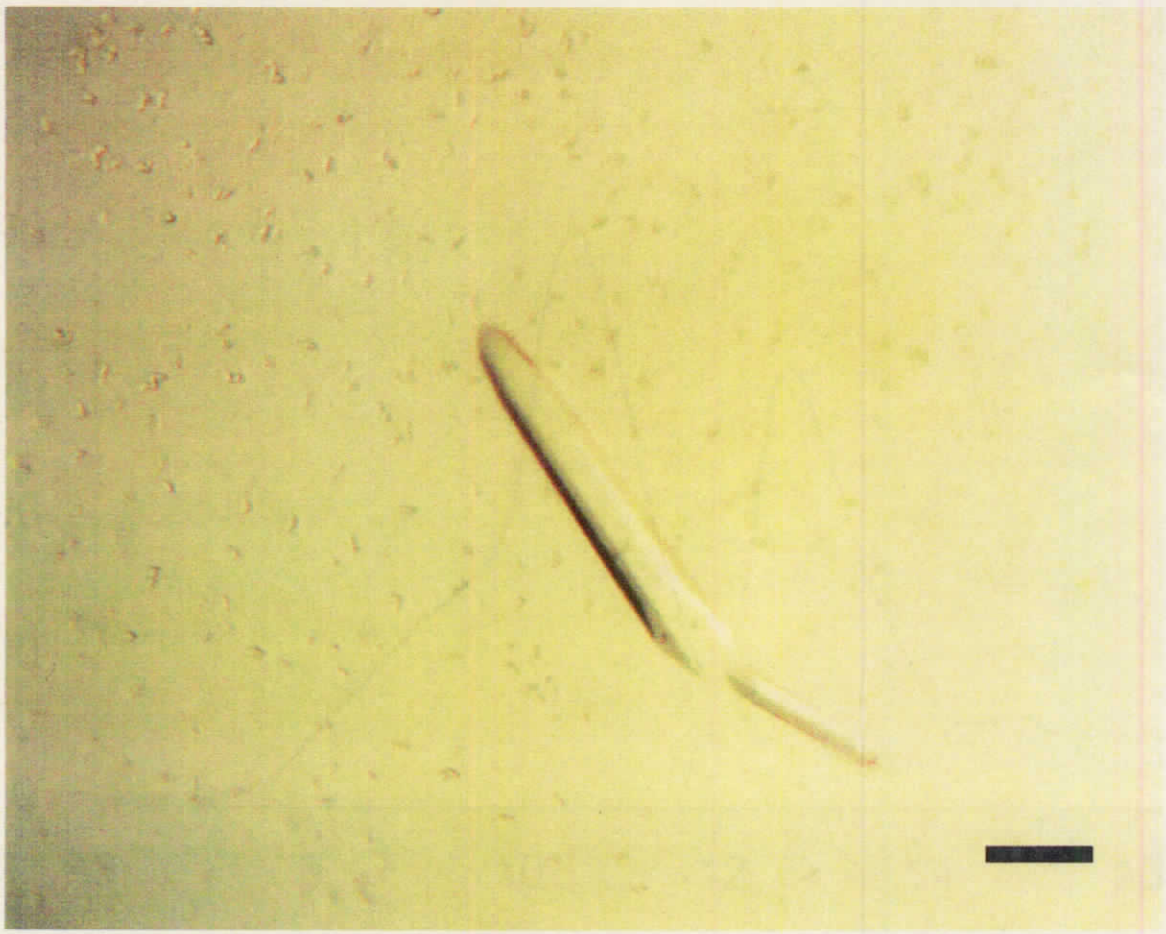

Figure 2-1

Crystal of SKD1. Its approximate dimensions are 0.05 x 0.05 x 0.35 mm^3. Bar shows 0.1 mm.

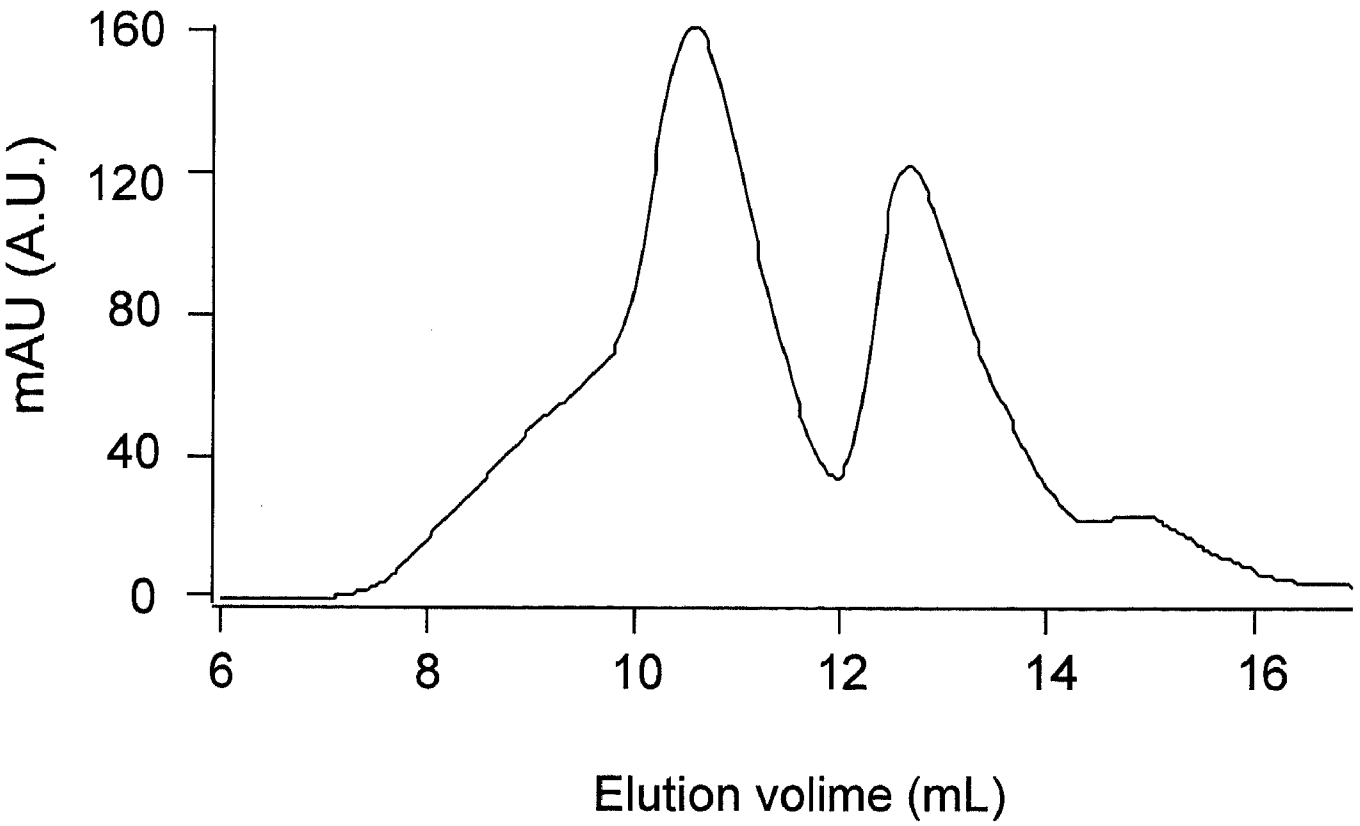

Figure 2-2

Elution profile of SKD1 in Superdex200. The former peak corresponds to an oligomeric moleculer weight size and the latter peak to monomer size in solution. A. U. means Arbitrary Unit.

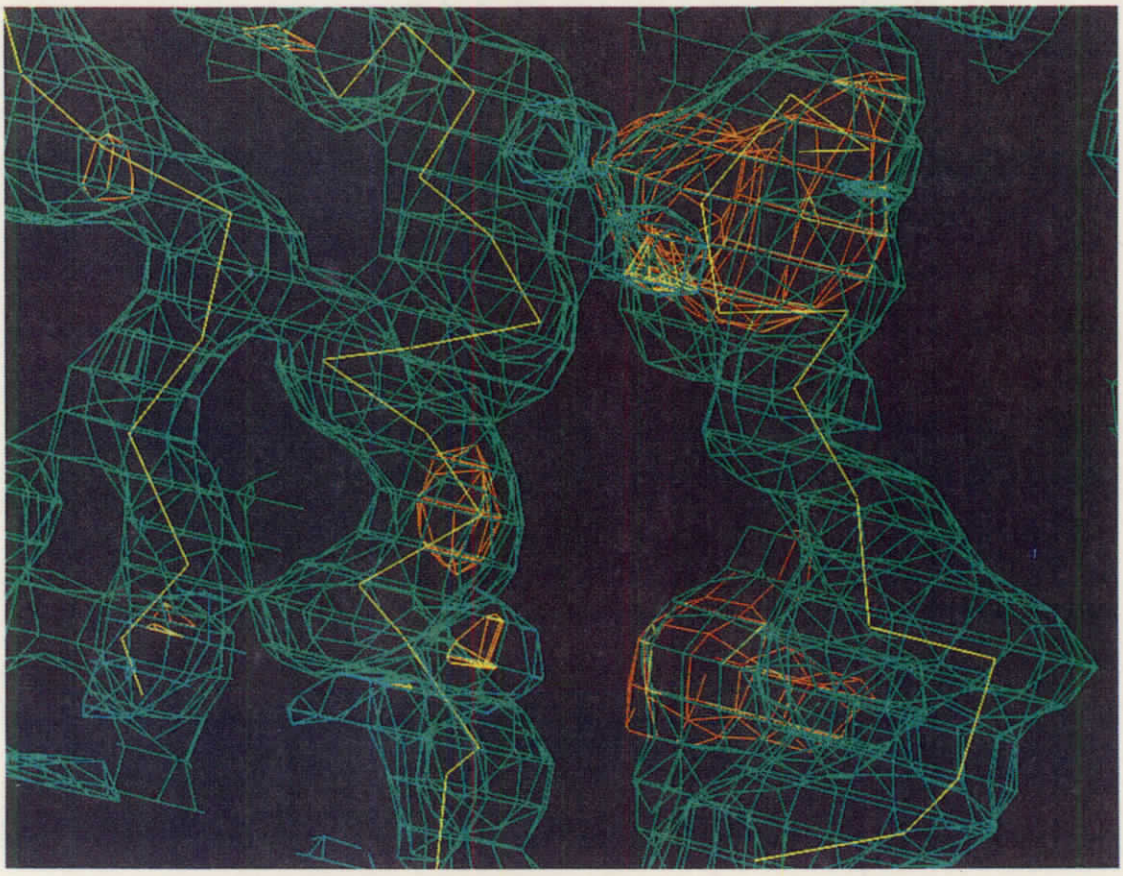

Figure 2-3

Electron density map of SKD1. α-helices section of 4 Å resolution first 2|Fo|-|Fc| map contoured at 1 σ (Blue) and |Fo|-|Fc| map contoured at 2 σ (Orange). Cα atom trace of SKD1 structure model shows yellow line.

A

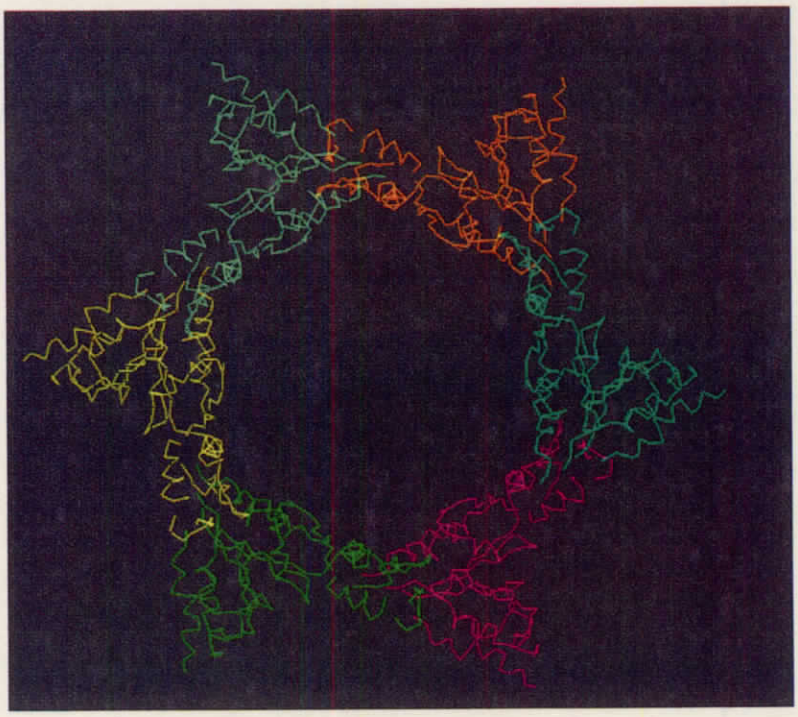

B

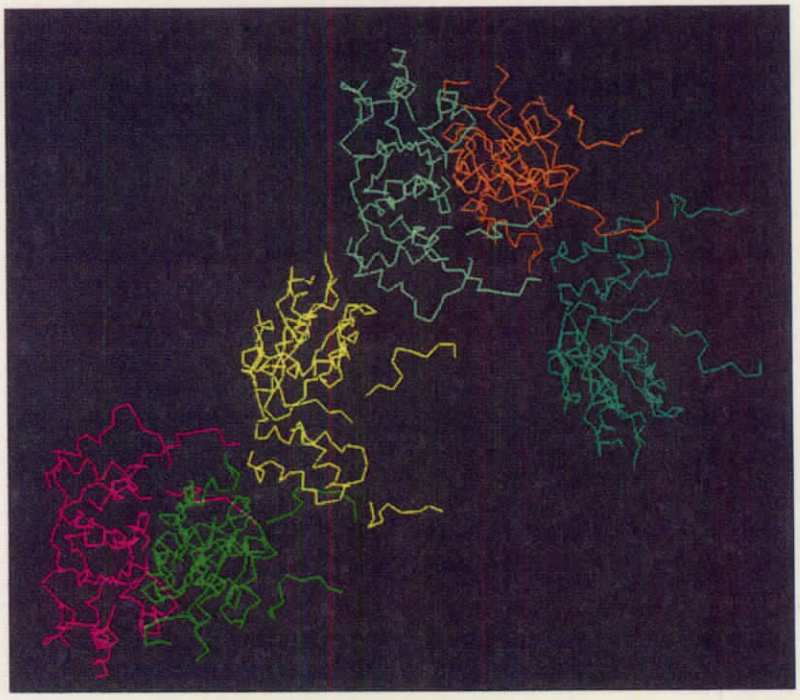

Figure 2-4

The primitive refinement model of SKD1 molecules in crystal. A) The location of SKD1 molecules from the top view. B) The location of SKD1 molecules from the side view. All SKD1 molecules are shown as Cα traces.

General conclusion

In this study, I researched the proteins related to the intra-cellular transport between Golgi apparatus and endosome and the endosomal transport. GGA1 related to clathrin-mediated transport was clearly shown the new knowledge below.

First, I determined the crystal structure of GGA1-GAE. In the crystal, GGA1-GAE forms an immunoglobulin-like β-sandwich fold composed of nine β-strands with one α-helix and exists as dimer faced anti-parallel on the other via a set of β-sheets (β3, 7 and 6). To elucidate the dimer formation of GGA1-GAE, small angle X-ray scattering of GGA1-GAE was measured. The obtained data shows GGA1-GAE also forms dimer in solution.

Surface plasmon resonance (SPR) experiment gave the interaction of GGA1-GAE with accessory protein peptides *in vitro*. GGA1-GAE binds to these accessory protein peptides at the order of 10- 100 μM. The interaction of GGA1-GAE with the GGA1 hinge peptide was also measured by SPR experiment. GGA1-GAE binds to the GGA1 hinge peptide at the order of 100 μM. The co-crystal structures of the GGA1-GAE/hinge and the GGA1-GAE/DDFGDF complexes were determined. The binding site of GGA1-GAE to the peptides is matched to the putative binding site from γ1-ear. Two phenylalanines of the peptide mainly interact with GGA1-GAE

hydrophobically in the GGA1-GAE/DDFGDF complex. The binding site is the same as that of the GGA1-GAE/DDFGDF complex and phenylalanine and tryptophan of the GGA1-hinge peptide are key residues for hydrophobic binding to GGA1-GAE. GGA1-GAE interacts with the GGA1-hinge peptide both *in vitro* and in crystal.

To elucidate the interaction of the GAE domain with the hinge region in GGA1, the quenching of tryptophan of the WNSF motif in the GGA1-hinge region were measured by the fluorescent experiment. I constructed a molecule containing the hinge region and the GAE domain substituted W444A and W636A, named GGA1-hinge—GAE. And I also constructed the other molecule which is additional substitution of K611Q for GGA1-hinge—GAE, named K611Q mutant GGA1-hinge—GAE. The fluorescence intensity of wild-type GGA1-hinge—GAE was less than that of K611Q mutant GGA1-hinge—GAE at the same concentration, which shows the environment around Trp382 of K611Q mutant GGA1-hinge—GAE is more hydrophilic than that of wild-type GGA1-hinge—GAE. The fluorescent intensity of wild-type GGA1-hinge—GAE was decreased under the existence of the DDFGDF peptide. The environment around Trp382 of wild-type GGA1-hinge—GAE is more hydrophilic when wild-type GGA1-hinge—GAE interacts with the DDFGDF peptide.

The GGA1 study determined the crystal structures of apo-form GGA1-GAE, the GGA1-GAE/hinge and the GGA1-GAE/DDFGDF complexes. I first analyzed the interaction of GGA1-GAE with the GGA1-hinge region both *in vitro* and in crystal. The binding site of GGA-GAE to the GGA1-hinge region is the same as that of GGA1-GAE to accessory proteins in crystal and each interaction competes to each other *in vitro*. The interaction of the GAE domain with the hinge region in GGA1 provides useful information to elucidate the function of GGA1 in clathrin-mediated transport, and the competition of the GGA1-hinge region and accessory proteins to GGA1-GAE will reveal the interaction networks of clathrin related proteins.

Second, I succeeded in the expression and purification of SKD1 recombinant related to endosomal transport. During purification, I found that SKD1 was two assemble condition in solution. And I succeeded in the crystallization of SKD1. Crystallographic analysis showed the possibility of SKD1 oligomer in crystal. From the crystallographic point of view, I think that SKD1 forms an oligomer to regulate the MVB sorting.

In this present study, I experimented GGA1 and SKD1 to understand clathrin-mediated transport and the MVB sorting. I analyzed structurally and functionally about GGA1-GAE and determined the new function on intra- or inter-

interaction of GGA1. I propose that GGA1 conformational change may regulate the clathrin-mediated transport. Crystallographically SKD1 can form an oligomer and I suggest that SKD1 may change the assembly condition from monomer to oligomer to regulate the MVB sorting.

Acknowledgements

The present work were carried out under the guidance of Professor Soichi Wakatsuki, The Graduate University for Advanced Studies, Structural Biology Research Center, Photon Factory, KEK, Japan, from 2002 to 2005.

The author is particularly grateful to express his sincere gratitude to Professor Soichi Wakatsuki for his giving the author a chance to study on this field, helpful suggestion, and continuous encouragement throughout this work. The author is also deeply grateful to Associate Professor Ryuichi Kato for his useful advice and continuous guidance. He is also grateful to Research Assistant Masato Kawasaki, Dr. Tomoo Shiba, and Reserch Assistant Yusuke Yamada for their stimulating discussion.

The author is grateful to Professor Mikio Kataoka and Research Assistant Hironari Kamikubo, Laboratory of Bioenergetics and Biophysics, Nara Institute of Science and Technology, for their assistance with the small angle X-ray scattering experiment. He also thanks the beamline staff at AR-NW12, PF, KEK, Japan and at BL-38B1, SPring-8, Japan for data collection facilities and support.

Special thanks are given to author's colaborater Professor Kazuhisa Nakayama, The Graduate School of Pharmaceutical Sciences, Kyoto University, for his continuous and fruitful cooperation. He wishes to thank all members of Structural Biology Research

Center, Photon Factory, KEK for their helpful assistance, occasional discussions, and profound interests.

Finally, the author wishes to express his thanks to his parents and friends for their understanding and hearty encouragement.